

**SYNTHESIS, STRUCTURAL CHARACTERIZATION
AND MESOMORPHIC PROPERTIES OF SCHIFF BASE
COPPER (II) COMPLEX**

NUR SYAZA SAHIRA BINTI AHMAD ZAIDI

**BACHELOR OF SCIENCE (Hons.) CHEMISTRY WITH
MANAGEMENT
FACULTY OF APPLIED SCIENCES
UNIVERSITY TEKNOLOGI MARA**

FEBRUARY 2023

**SYNTHESIS, STRUCTURAL CHARACTERIZATION AND
MESOMORPHIC PROPERTIES OF SCHIFF BASE COPPER (II)
COMPLEX**

NUR SYAZA SAHIRA BINTI AHMAD ZAIDI

**Final Year Project Report Submitted in
Partial Fulfilment of the Requirements for the
Degree of Bachelor of Science (Hons.) Chemistry with Management
in the Faculty of Applied Sciences**

FEBRUARY 2023

This Final Year Report Project entitled **“Synthesis, Structural Characterization and Mesomorphic Properties of Schiff Base Copper (II) Complex”** was submitted by Nur Syaza Sahira Binti Ahmad Zaidi, in partial fulfilment of the requirement for Degree of Bachelor of Science (Hons.) Chemistry with Management, in the Faculty of Applied Science, and was approved by



Dr Yanti Yana Halid
Supervisor
B. Sc. (Hons.) Chemistry with Management
Center for Applied Sciences Studies
Universiti Teknologi MARA Cawangan Sarawak
93400 Kota Samarahan
Sarawak



Nurhafizah Binti Mohd Selihin
Project Coordinator
B. Sc. (Hons.) Chemistry with
Management
Center for Applied Sciences Studies
Universiti Teknologi MARA
Cawangan Sarawak
93400 Kota Samarahan
Sarawak



Ts. Dr. Siti Kartina Binti Abdul Karim
Head
Center for Applied Sciences Studies
Universiti Teknologi MARA
Cawangan Sarawak
93400 Kota Samarahan
Sarawak

Date: 27 FEBRUARY 2023

TABLE OF CONTENTS

	Page
TABLE OF CONTENTS	iii
LIST OF TABLES	v
LIST OF FIGURES	vi
LIST OF SYMBOLS	viii
LIST OF ABBREVIATIONS	ix
ABSTRACT	x
ABSTRAK	xi
ACKNOWLEDGEMENTS	xii
CHAPTER 1	1
1.1 Background	1
1.2 Problem statement	4
1.3 Significance of study	5
1.4 Objective of study	6
CHAPTER 2	7
2.1 Introduction	7
2.2 Liquid Crystal	7
2.3 Metallomesogen	13
2.4 Schiff base ligand	19
2.5 Schiff base metal complexes	23
2.5.1 Copper (II) Schiff base metal complexes	25
CHAPTER 3	30
3.1 Materials	30
3.2 Apparatus	30
3.3 Instrumentation	31
3.4 Methods	32
3.4.1 Synthesis of Schiff base ligand (H ₂ L)	32
3.4.2 Synthesis of Copper (II) Complex (CuL)	32
3.4.3 Synthesis of elongated Copper (II) Complexes (CuLC ₁₀)	33
3.5 Instrumental Analysis	34
3.5.1 Nuclear magnetic resonance (NMR)	34
3.5.2 FTIR-spectroscopy	34
3.5.3 UV-Vis-spectroscopy	35
3.5.4 Magnetic susceptibility	35
3.5.5 Thermogravimetric analysis (TGA)	36

3.5.6	Differential scanning calorimetry (DSC)	36
3.5.7	Optical polarized microscopy (OPM)	37
CHAPTER 4		38
4.1	Introduction	38
4.2	Structure elucidation of H ₂ L Schiff base ligand	39
4.3	Structure elucidation of CuL	42
4.4	Structure elucidation of CuLC ₁₀	46
CHAPTER 5		55
5.1	Conclusion	55
5.2	Suggestion for future works	59
CITED REFERENCES		62
<i>CURRICULUM VITAE</i>		66

LIST OF TABLES

Table	Caption	Page
2.1	The ^1H -NMR data and peak assignments for free Schiff base ligand, H_2L .	41

LIST OF FIGURES

Figure	Caption	Page
2.1	The comparison of molecular arrangement of solid, liquid and liquid crystal (Malik et al., 2022).	8
2.2	Categorization of Liquid Crystal (Bala et al., 2021)	10
2.3	Liquid crystals mesophases molecule alignment, (a) nematic, (b) cholesteric, (c) smectic A, (d) smectic C, & (e) columnar (Malik et al., 2022).	12
2.4	The schematic phase diagram of lyotropic liquid crystal (Dierking, 2019).	13
2.5	The example of nematic metallomesogen mesophase under OPM (Parker et al., 2021).	15
2.6	The example of smectic mesophase under OPM, (a) SmA (b) SmC (Cuerva et al., 2021b).	16
2.7	Example of columnar mesophase observed under OPM (Cuerva et al., 2021b).	17
2.8	The general structure of Schiff base (R1=hydrogen, alkyl or aryl, R2 and R3 = alkyl or aryl) (Raczuk et al., 2022).	19
2.9	The general synthesis of Schiff base ligand (Sadia et al., 2021).	20
2.10	Examples of Schiff bases with the imine fragments are framed (Raczuk et al., 2022).	20
2.11	Structure of Schiff base Ligand L (Sadia et al., 2021).	22
3.1	Structural formula of (a) 2,4-dihydroxybenzaldehyde, (b) ethylenediamine, (c) Schiff base ligand (H ₂ L).	32
3.2	Synthesis of Cu (II) complex (CuL), the structure (c) Schiff base ligand (H ₂ L) (d) Copper (II) Acetate monohydrate and (e) proposed structure of Cu (II) complex (CuL).	33
3.3	Synthesis of elongated Cu(II) complex (CuLC ₁₀) and structure	

	of (e) proposed structure of Cu (II) complex (CuL), (f) 1-bromodecane and proposed structure of (g) elongated Copper (II) complex (CuLC ₁₀).	34
4.1	FTIR spectra for free ligand H ₂ L.	40
4.2	¹ H-NMR spectra for free Schiff base ligand H ₂ L.	41
4.3	Proposed structure for free Schiff base ligand H ₂ L	42
4.4	FTIR spectra for CuL complex	44
4.5	UV-Vis spectra for CuL complex	45
4.6	Proposed structure for CuL complex	45
4.7	FTIR spectra for CuLC ₁₀ complex	47
4.8	UV-Vis spectra for CuLC ₁₀ complex	48
4.9	TGA of CuLC ₁₀ complex	50
4.10	DSC of CuLC ₁₀ complex	51
4.11	Photomicrographs for CuLC ₁₀ complex on: (a) heating at room temperature at 30°C; (b) heating at 60°C and (c) heating at 86°C with 50x magnification	52
4.12	Photomicrographs for CuLC ₁₀ complex on: (a) heating at room temperature at 100°C; (b) heating at 150°C; (c) heating at 180°C. and (d) heating at 200°C	53
4.13	The suggested structure for CuLC ₁₀ complex	54
5.1	The suggested structure for Cu(II) complex with long alkyloxy chain substitute as a long alkyl chain tail for the complex by synthesis reaction of Cu(II) complex with 1-bromodecane	59

LIST OF SYMBOLS

Symbols		Page
A	Absorbance	18
ϵ	Molar absorption coefficient	18
b	Optical pathlength	18
c	Molar concentration	18
δ	Chemical Shift	21
Δ	Delta (Change in value)	43
ϵ_{max}	Molar absorptivity at highest absorbance	44
λ_{max}	Highest absorbance	44
μ_{eff}	Effective magnetic moment	48

LIST OF ABBREVIATIONS

NMR	:	Nuclear Magnetic Resonance
FTIR	:	Fourier Transform Infrared
TGA	:	Thermogravimetric Analysis
DSC	:	Differential Scanning Calorimetry
UV-Vis	:	Ultraviolet-Visible spectroscopy
OPM	:	Optical Polarized Microscopy
Cu	:	Copper
H ₂ L	:	Schiff base ligand
CuL	:	Cu(II) complex with Schiff base ligand
CuLC ₁₀	:	Cu(II) complex with Schiff base ligand that bind with long alkyloxy chain
DMSO	:	Dimethyl sulfoxide
HCl	:	Hydrochloric acid
DMF	:	Dimethylformamide
Ni	:	Nickel
L	:	Ligand

ABSTRACT

SYNTHESIS, STRUCTURAL CHARACTERIZATION AND MESOMORPHIC PROPERTIES OF SCHIFF BASE COPPER (II) COMPLEX

Metallomesogens are metal-containing liquid crystals. There is little known about metallomesogens derived from short-chain Schiff base ligands and long alkoxy groups. This research aims to learn more by developing a new metallomesogen with a short chain spacer and a substituent with a long alkoxy group that can be used to make low-cost electronic devices. The main objective of this research project was to synthesis and characterized the structure of Schiff base ligand and its Cu(II) complexes (CuL and CuLC₁₀), and study the thermal stability and mesomorphic behaviour for the Cu(II) complex. In this study, Cu(II) complex (CuL) and its Schiff base ligand (H₂L) were successfully synthesized by using ethanol as a solvent. Besides, a new metallomesogen derived from salen Schiff base ligand with two carbon chain substituent with the long terminal end alkoxy group (decane) coordinated with Cu(II) metal (CuLC₁₀) was also synthesized by reacting Cu(II) complex (CuL) with 1-bromodecane in ethanol as solvent by refluxing for 4 hours. The structure of Schiff base ligand (H₂L) was characterized by using FTIR and ¹HNMR spectroscopy while its complexes (CuL and CuLC₁₀) was characterized by using FTIR spectroscopy and the geometry of the metal centre was determined by using UV-Vis spectroscopy. As for the thermal properties, magnetic properties, and mesomorphic properties studies of the Cu(II) complex, CuLC₁₀ were conducted using TGA, magnetic susceptibility and DSC as well as OPM instrumental analysis respectively. Based on the FTIR spectroscopy, both Cu(II) complexes (CuL and CuLC₁₀) shows the existence of acetate ion (CH₃COO⁻) in chelating binding mode. The UV-Vis for both complexes indicate the geometry of the metal centre of square planar. As for the Cu(II) complex of CuLC₁₀ was expected to have mesomorphic properties and perhaps with high thermal stability. However, the synthesized Cu(II) complex (CuLC₁₀) in this research project does not shows any mesomorphism properties and have thermal stability only up to 64°C based on the TGA, DSC and OPM analysis studies. This is because the CuLC₁₀ complex shows no coordination of the CuL with long alkyloxy chain based on the analysis of FTIR and TGA data. Furthermore, the study using magnetic susceptibility instrumental analysis shows that the CuLC₁₀ complex is paramagnetic and a dinuclear complex which contain two Cu(II) metal centres. Thus, the Cu(II) complex, CuLC₁₀ contain two Cu(II) metals as metal centres that bind with two acetate ion in chelating binding mode but the complex does not exhibit mesomorphism behaviour and have low thermal stability may be due to no coordination of the complex with long alkyloxy chain tail as its substitute which causing the structure of the complex to be rigid but not elongated.

ABSTRAK

SINTESIS, CIRI-CIRI STRUKTUR DAN SIFAT-SIFAT MESOMORFIK *SCHIFF* BASE KUPRUM(II) KOMPLEKS

Metallomesogen ialah kristal cecair yang mengandungi logam. Terdapat sedikit yang diketahui tentang metallomesogen yang diperolehi daripada ligan asas Schiff rantai pendek dan kumpulan alkoxi panjang. Penyelidikan ini bertujuan untuk menghasilkan metallomesogen baru dengan ligan asas Schiff rantai pendek dan substituen dengan kumpulan alkoxi panjang yang boleh digunakan untuk membuat peranti elektronik kos rendah. Objektif utama projek penyelidikan ini adalah untuk mensintesis dan mencirikan struktur ligan asas Schiff dan kompleks Cu(II)nya (CuL dan CuLC₁₀), dan mengkaji kestabilan termal dan tingkah laku mesomorfik bagi kompleks Cu(II). Dalam kajian ini, kompleks Cu(II), (CuL) dan ligan asas Schiffnya (H₂L) berjaya disintesis dengan menggunakan etanol sebagai pelarut. Selain itu, metallomesogen baharu yang diperolehi daripada ligan asas salen Schiff dengan dua substituen rantai karbon hujung terminal panjang dengan kumpulan alkoxi (decane) yang diselaras dengan logam Cu(II) (CuLC₁₀) turut disintesis dengan melakukan tindak balas kompleks Cu(II) (CuL) dengan 1-bromodecane dalam etanol sebagai pelarut dengan refluks selama 4 jam. Struktur ligan asas Schiff (H₂L) dicirikan dengan menggunakan FTIR dan ¹H-NMR spektroskopi manakala kompleksnya (CuL dan CuLC₁₀) dicirikan dengan menggunakan FTIR dan geometri pusat logamnya ditentukan dengan menggunakan spektroskopi UV-Vis. Bagi kajian sifat termal, sifat magnet dan sifat mesomorfik kompleks Cu(II), CuLC₁₀ telah dikaji menggunakan analisis instrumental TGA, kecenderungan magnetik dan DSC serta OPM. Berdasarkan spektroskopi FTIR, kedua-dua kompleks Cu(II) menunjukkan kewujudan ion asetat (CH₃COO⁻) dalam mod pengikatan. UV-Vis untuk kedua-dua kompleks menunjukkan geometri pusat logam bagi satah segi empat sama. Bagi kompleks Cu(II), CuLC₁₀ dijangka mempunyai sifat mesomorfik dan mungkin dengan kestabilan haba yang tinggi. Bagaimanapun, kompleks Cu(II) yang telah disintesis (CuLC₁₀) dalam projek penyelidikan ini tidak menunjukkan sebarang sifat mesomorfisme dan mempunyai kestabilan terma hanya sehingga 64°C berdasarkan kajian analisis TGA, DSC dan OPM. Ini kerana kompleks CuLC₁₀ tidak menunjukkan koordinasi CuL dengan rantai alkyloxy yang panjang berdasarkan analisis data FTIR dan TGA. Tambahan pula, kajian menggunakan analisis instrumental kerentanan magnet menunjukkan kompleks CuLC₁₀ adalah paramagnet dan kompleks dinuklear yang mengandungi dua pusat logam Cu(II). Oleh itu, kompleks Cu(II), CuLC₁₀ mengandungi dua logam Cu(II) sebagai pusat logam yang mengikat dengan dua ion asetat dalam mod pengikatan tetapi kompleks tidak menunjukkan tingkah laku mesomorfisme dan mempunyai kestabilan haba yang rendah mungkin disebabkan oleh tiada koordinasi kompleks dengan ekor rantai alkiloksi yang panjang sebagai penggantinya yang menyebabkan struktur kompleks menjadi tegar tetapi tidak memanjang.

ACKNOWLEDGEMENTS

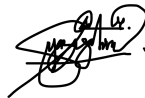
Frist praise is to Allah, the Almighty, on whom ultimately we depend for sustenance and guidance. Second, I would like to acknowledge and express my sincere gratitude to the following people and institutions for significant role in enabling me to complete my Final Year Project.

My sincere appreciation and highest gratitude goes to my supervisor, Dr Yanti Yana Binti Halid for thoughtful advice, constant encouragement and patience in guiding me throughout this whole project. Without her I would not be able to complete my research report as too much knowledge I had gained from her in the journey of completing my report.

Next, sincere thanks to all the laboratory staffs for the help, encouragement, cooperations and constructive suggestions they have given to me.

My sincere appreciation goes to my close friends and postgraduates students for giving me moral supports, loves and always being there for me whenever I need help to complete my research.

Lastly, my deepest thanks and highest gratitude to my family, especially my parents for the loves, financial support and always be there for me whenever I face some hardship throughout this project.



Nur Syaza Sahira Binti Ahmad Zaidi

CHAPTER 1

INTRODUCTION

1.1 Background

Liquid crystals are material that possessed both liquid and crystalline solid at the same time. Thermotropic liquid crystals and lyotropic liquid crystals are two subcategories of organic liquid crystals. These subcategories are differentiated from one another by the fact that thermotropic liquid crystals are affected by changes in temperature, while lyotropic liquid crystals are affected by changes in concentration. As for liquid crystals that contain metal, these are referred to as metallomesogens, and the study of metallomesogens is a well-established field that has captured the attention of researchers over the past two decades due to the unique properties that they exhibit, including electro-optic responses and polymorphic behaviour. Besides, Metallomesogen is a metal complex that acts and has properties that are mesomorphic. These properties are what make metallomesogen different from other metal complexes. As for mesomorphic properties are defined as the ability of a material to contain both liquid and solid phases at the same time at a given temperature, which are very useful properties for electronic displays because liquid crystal molecules can control the amount,

colour, and direction of light vibration through them by manipulating the alignment of their molecules. These mesomorphic properties of a material can be induced depending on the structure of the ligand and how it coordinated to certain metals. Daniel Vorlander, a scientist, is credited with making the initial discovery of the metallomesogen in the year 1923 (Pelzl et al., 2001). The capability of metal ions to form the various coordination geometries, which offer metallomesogen molecules with a wide range of mesomorphic characteristics and properties. The incorporation of a particular metal ion into the structure in order to produce a particular metallomesogen enables the compounds to display the properties of the metal ion centres, such as high coordination bond polarity, a diverse range of oxidation states, a variety of geometrical shapes, a range of colours, redox behaviour, and magnetism (Aswini Krishna et al., 2019). Due to their special property shared with their metal centres and their capacity to combine the fluidic state of mesophases with qualities like photo and electroluminescence, metalomesogen can behave as multifunctional materials (Cuerva et al., 2021a). As a result, there will be entirely new and exciting opportunities in optoelectronics, energy, the environment, biomedicine, and a variety of other fields yet to be discovered. Therefore, scientists are motivated to study and synthesizing a wide variety of metallomesogens with diverse of features and applications.

Metallomesogens that are studied the most are metal complexes that are synthesized from salicyldiimine Schiff base ligands (Halid, 2016). Synthesization of Schiff bases can be achieved by the condensation reaction of a primary amine with the carbonyl compounds, which can be either aldehyde or ketones under the reaction condition of acid or base catalyst or heating (Sadia et al., 2021). It is named after its discoverer, Hugo Schiff (Raczuk et al., 2022). The synthesis and preparation of the ligand is a critical step in constructing new complexes because the properties of the ligand contribute to the properties of the metal complexes as a whole. The properties of the Schiff bases ligand, such as the structural-functional groups, electron donor, and ligand position in the coordination area in the coordination complex, will play a significant role in determining the metal complex properties. Schiff bases are ligands that coordinate to metal ions via the azomethine nitrogen, but the azomethine group does not have the necessary strength to form a stable complex with metal ions. Therefore, it is possible to produce more stable compounds by employing a functional group as a substituent in the Schiff base, such as a hydroxyl group (Halid, 2016). Because of their ease of synthesis, availability, and electronic properties, Schiff base ligands have received a lot of attention in the field of coordination chemistry (More et al., 2019). Schiff bases have found widespread application in the dye industry, catalysis, fungicides, and agrochemicals. Several Schiff bases have been found to have powerful antibacterial, antifungal, antiviral, and anticancer properties (More et al., 2019). Aside from that, because of their photochromic properties, Schiff

base ligands are excellent compounds used as photostabilizers, solar filters, optical sound recording technology, and even solar collector dyes. Schiff bases and its metal complexes, such as metallomesogen containing Schiff base ligand are still being actively studied in order to see improvements in the future.

In this project was focused on the synthesis and structural characterization of Cu(II) complexes with its salen Schiff base ligand. The mesomorphic properties of both Schiff base ligand and the Cu(II) Schiff base complex was studied by using the Thermogravimetric Analysis (TGA), Differential Scanning Calorimetry (DSC), Magnetic Susceptibility and Optical Polarized Microscopy (OPM). As for the structure elucidation of the Schiff base ligand will was analyzed by using FTIR and ¹H-NMR spectroscopies while its Cu(II) complex was studied by using FTIR and UV-Vis spectroscopies.

1.2 Problem statement

This study will contribute new knowledge on research and add to our understanding of metallomesogens. Based on similar studies involving the salen type of Schiff base ligand, no study proposes for the short-chain Schiff base ligand such as two-carbon chain substituent with the long terminal end

alkoxy group such as decane (ten carbon chain) coordinated with Cu(II) acetate monohydrate to form a metal complex. Besides, most studies on metallomesogen complexes are found to have low thermal stability and high melting point, which limit the study on the physical properties of the metallomesogen. In this report, the carbon chain spacer of the salen type Schiff base ligand was shorter and the carbon chain of terminal end alkoxy group was longer than in the previous study, which used Schiff base ligand with an eight-carbon chain and a tert-butyl terminal end group. The shorter Schiff base ligand carbon chain spacer and the longer carbon chain terminal end alkoxy group of the ligand were expected to give a more rigid yet elongated structure of metal complex, resulting in a new metallomesogen and improved mesophase properties and characteristics.

1.3 Significance of study

Metallomesogen is a liquid crystal that contains metal ions, especially *d* (transition metal) blocks, which can be derived with various ligands such as monodentate, bidentate, and polydentate ligands. Over the last two decades, studies in this area have contributed to our understanding of the synthesis of mesomorphic compounds with more desirable and improved properties, such as by using the elongated but rigid structure of Schiff base ligand and using a different kind of metals either from transition metal group or lanthanide group. This report was investigated metallomesogens, which

contain transition metal ions from the first row of the transition metal with one or more unpaired electrons and were thought to have potential in photonic materials, semiconductors, and optoelectronic devices. This is an exciting and challenging area that contributes so much knowledge in coordination chemistry that is important for scientific and industrial applications such as in the manufacturing of electronic devices, including diodes, television and much more. Thus, the study was aims to create a future metallomesogen compound by using a salen type Schiff base ligand containing diimine and aromatic groups to induce mesomorphism and a transition metal ion such as Cu as a metal central that was expected to improve thermal stability and electrical conductivity while also providing low melting point metallomesogen properties. The metallomesogen that was synthesized in this study were expected to become a material with future applications that can be used as semiconductors and low-cost optoelectronic devices.

1.4 Objective of study

1. To synthesize and characterize Schiff base ligand and its Cu(II) complexes structures by using ^1H NMR and FTIR spectroscopies.
2. To determine the thermal stability and magnetic properties of the Cu(II) complex by using TGA and magnetic susceptibility.
3. To study the mesomorphic properties of Schiff base Cu(II) complex by using TGA, DSC and OPM.

CHAPTER 2

LITERATURE REVIEW

2.1 Introduction

The key point of this research project is to synthesize and characterize the structure of Schiff base ligand and its Cu(II) complex as a metallomesogen with a longer terminal end alkoxy group. There are not many studies have been done on metallomesogens made by combining short-chain Schiff base ligands with long alkoxy groups. This study help add new knowledge on metallomesogens by investigating a short-chain Schiff base ligand with a long terminal end alkoxy group coordinated with Cu(II) acetate monohydrate to form a metal complex which is expected to result in a more rigid and elongated structure of metal complex, leading to a new metallomesogen with improved mesophase properties and characteristics that can be use as semiconductors and low-cost optoelectronic devices.

2.2 Liquid Crystal

Liquid crystals are fluid materials in the naked eyes but crystalline under a polarised microscope. It also materials with a state of matter that possesses

both liquid and crystalline solid properties at the same time. Liquid crystals have anisotropic properties, which means that their molecules tend to point in the same direction as the axis (Halid, 2016). This distinguishes liquid crystals from liquid phases, which have no inherent molecular order, and solid phases, which contain highly ordered molecules. The anisotropic properties of liquid crystal molecules cause this unique material to have less order than solid or crystal phase molecules but more order than liquid phase molecules, causing liquid crystals to flow like liquids but imitate the crystalline state under the polarising microscope. Due to its unique dual state of matter which has viscous properties such as fluidity, droplet formation, and mechanical properties, as well as solid crystalline properties such as periodic and anisotropic properties; thus, they are referred to as mesophases (Malik et al., 2022). The comparison of solid, liquid and liquid crystal molecular arrangement is shown in Figure 2.1.

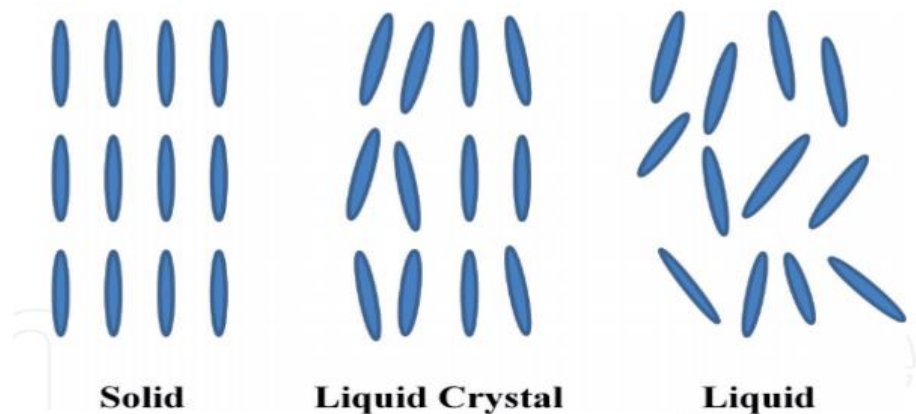


Figure 2.1 The comparison of molecular arrangement of solid, liquid and liquid crystal (Malik et al., 2022).

Liquid crystals are distinguished from other solid-state materials by the ease with which they react to extraneous stimuli such as surfaces, light, heat, mechanical force, or electric and magnetic fields. In addition to this, liquid crystals have the ability to self-heal, which allows them to eliminate any imperfections that may occur (Carlescu, 2019). The liquid crystal phase was first discovered in 1888 by an Austrian scientist named Friedrich Reinitzer when he discovered a material that has two different melting points which known as cholesteryl benzoate by manipulating the temperature of the sample and noticing the changes that occurred (Malik et al., 2022). Since then, Friedrich Reinitzer being noticed as a discoverer of the new state phase of matter and from that liquid crystal gained interest from multi-disciplinary research fields including chemistry, physics and even from mathematics, biology, engineering, biotechnology and much more.

Liquid crystals are divided into two main categories which are thermotropic and lyotropic liquid crystals as shown in Figure 2.2. These categories describe liquid crystal phases based on their positional order or orientation as a result of external variables such as temperature and concentration. Thermotropic liquid crystals produce various types of mesophases due to temperature variations, and these transitions are thermally controlled. The mechanism divides into two types of thermotropic liquid crystals that are enantiotropic liquid crystals, which can be formed by either decrease the liquid temperature or increase the solid temperature, and monotropic liquid

crystals, which can be formed by either increase the temperature of a solid-state material or decrease the temperature of a liquid-state material in order to form an aligned and arranged liquid crystal arrangement (Malik et al., 2022).

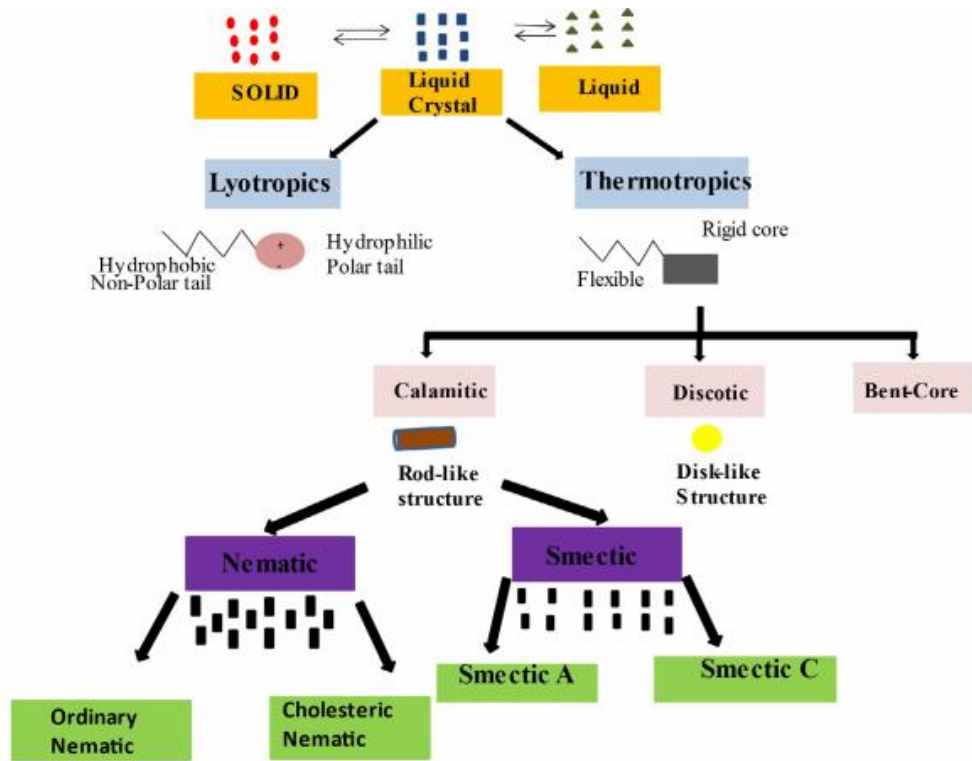


Figure 2.2 Categorisation of Liquid Crystal (Bala et al., 2021).

Thermotropic liquid crystals have different types of mesophases which are rod-like (calamitic), disc-like (discotic) and Bent core polycatenar (have many tailed). Calamitic mesophase can further be divided into main categories of mesophases which are nematics, cholesteric and smectics while, columnar mesophse can be divided into the disc-like type of mesophase. Nematic mesophase is the basic liquid crystal phase where its

molecular alignment is closely linked with local molecular axis orientation which can be influenced by external factors such as an electric field that assist the molecular axis to align accordingly (Malik et al., 2022). The cholesteric mesophase state is similar to the nematic state, where each has nematic layers with its own directors. Smectic mesophases are positioned in layers and have long axes that point in approximately a similar direction (Ula et al., 2018). Smectic can be broken down into three different varieties: smectic A, smectic B, and smectic C. Out of these three forms, smectic A and smectic C are the most prevalent. As for columnar mesophases, it is arranged in a 2D pattern and its molecules are characterized based on their packing motives and this mesophase is also known as discotic liquid crystals because its molecular structure resembles a disc and is stacked in a column form (Malik et al., 2022). Figure 2.3 below shows the alignment of the molecule of liquid crystals mesophases.

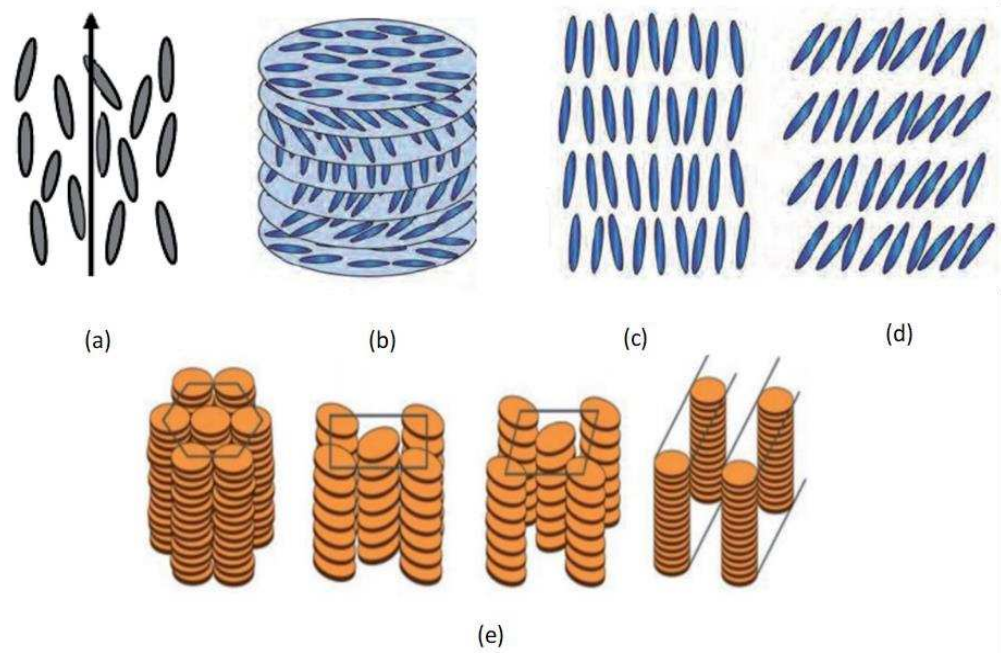


Figure 1.3 Liquid crystals mesophases molecule alignment, (a) nematic, (b) cholesteric, (c) smectic A, (d) smectic C, & (e) columnar (Malik et al., 2022)

Lytotropic liquid crystals are produced from a mixture of surfactants, water and co-surfactants. These lyotropic liquid crystals are liquid crystals that formed when amphiphilic molecules are dissolved in a suitable solvent at the appropriate temperature and concentration and are known to be a self-assembled mesophase (Bala et al., 2021). However, lyotropic liquid crystal is different from thermotropic liquid crystal because it is affected by the concentration of the amphiphilic molecules in a solvent. When the concentration of amphiphilic molecules is low, micelles will be formed in which the polar molecular head will be directed towards water molecules, resulting in a liquid isotropic phase (Bala et al., 2021). As the concentration increase, these micelles will form well-ordered structures and can form

cubic phases followed by hexagonal phases, and then lamellar phases, as well as inverted phase nanomaterials when it is at even higher concentration (Dierking, 2019). The schematic phase diagram of lyotropic liquid crystal is shown in Figure 2.4.

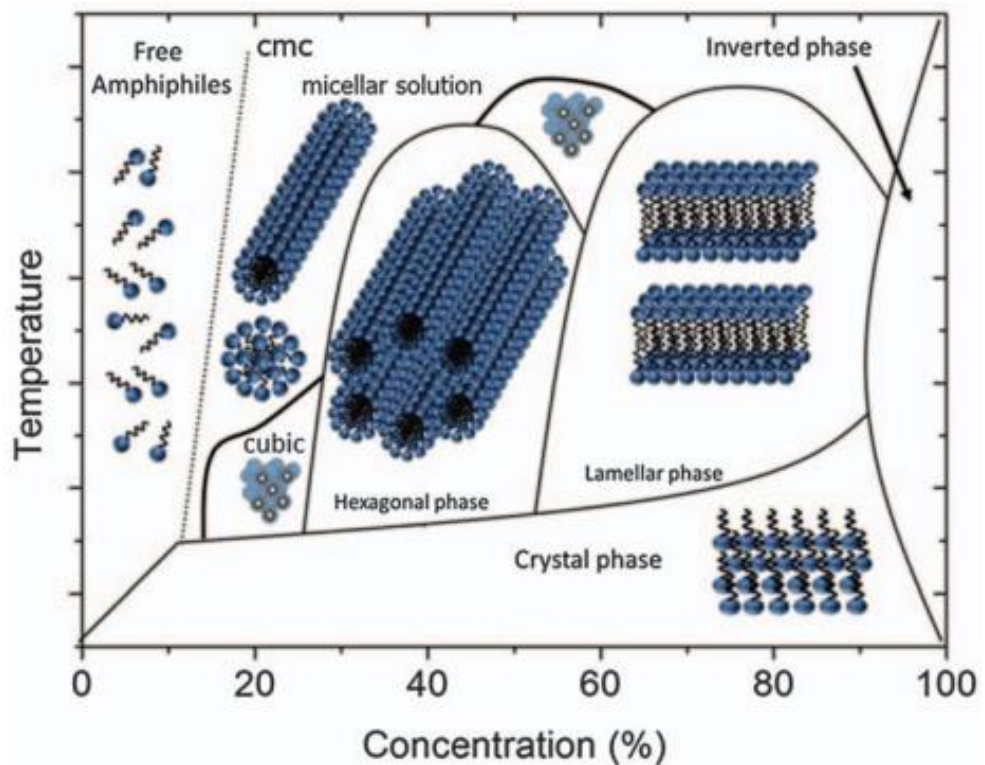


Figure 2.4 The schematic phase diagram of lyotropic liquid crystal (Dierking, 2019).

2.3 Metallomesogen

Metallomesogens are metal complexes which having liquid crystalline properties and also possess many types of mesophases similar to organic liquid crystals. The metallomesogen can be said as a very well-known field

and gained so much interest in science due to its electro-optic responses and polymorphic behaviour. The first metallomesogen was discovered by a scientist named Daniel Vorländer in the year of 1923 when he examined the Schiff base-mercury mesogens (Pelzl et al., 2001). Metallomesogens are distinguished from organic liquid crystals by the variety of molecular geometry that can be formed when metal is introduced into a chemical structure. By incorporating a particular metal ion into its structure, metallomesogen has the potential to take on the properties of a metal ion, including the high polarity of its coordination bonds, a diverse range of oxidation states, a variety of geometrical shapes, colour, redox behaviour, and magnetic properties (Aswini Krishna et al., 2019). Besides, because of its one-of-a-kind property that is shared by metal ions and its ability to combine the fluidic state of mesophase with properties such as photo and electroluminescence, metallomesogen can also behave as multifunctional materials and offers new and exciting opportunities in the fields of optoelectronics, energy, the environment, and biomedicine (Cuerva et al., 2021a).

Metallomesogens are similar to organic liquid crystals where they also exhibit the thermotropic mesophase. Unlike organic liquid crystals, thermotropic metallomesogens have been created by combining many metals, especially *d* (transition metal) blocks with different types of ligands such as monodentate, bidentate and polydentate ligands. Under

thermotropic metallomesogens can show calamitic (rod-like), discotic (disk-like) and polycatenar (many tailed) mesophases (Halid, 2016).

The calamitic mesophase of metallomesogen is further subdivided into nematic and smectic mesophases. Nematic metallomesogen mesophase is similar to organic liquid crystal where it is a metallomesogen with a molecular alignment that tends to align in the same direction as the axis but no particular molecular order. Nematic metallomesogens are extremely useful materials due to their high birefringence, low electric field frequency sensitivity, and highly flexible structure. The properties of birefringence of nematic metallomesogen are caused by polarised light, and it is also capable of reorientation due to anisotropy in the electrical charge distribution across the molecule. Furthermore, the electric field can help the molecular axis to align accordingly in nematic metallomesogen. The example of nematic mesophase under OPM can be seen in Figure 2.5.

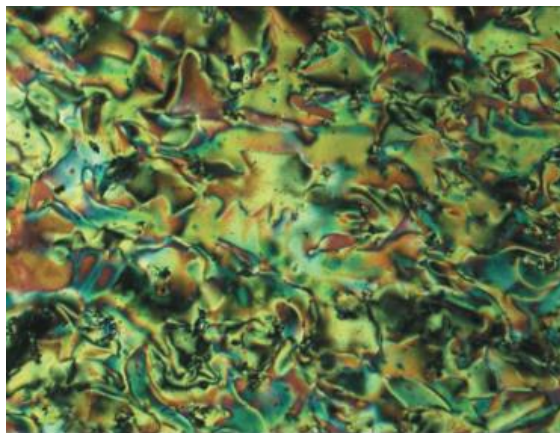


Figure 2.5 The example of nematic metallomesogen mesophase under OPM (Parker et al., 2021).

In terms of molecular alignment, smectic metallomesogen phase is also similar to smectic phase of organic liquid crystal. Smectic mesophases are aligned similarly to nematic phases in that they have long axes that point in roughly the same direction as the axis, but they are positioned in layers (Ula et al., 2018). Aside from that, being similar to smectic of liquid crystal, metallomesogen also has three types of smectic mesophases which are smectic A, B, and C. However, Smectic A (SmA) and Smectic C (SmC) are the two most prevalent varieties of smectic mesophases for metalomesogen that have mostly been discovered. Many compounds exhibit more than one type of smectic phase. The molecular alignment in SmA mesophase shows the director are perpendicular to the smectic plane, and the molecules have no specific positional order. The molecular alignment of SmC is the same as that of SmA, but its director will have a constant tilt angle measured typically to the smectic plane, which distinguishes it from SmA. The example of SmA and SmC mesophase under OPM can be shown in Figure 2.6.

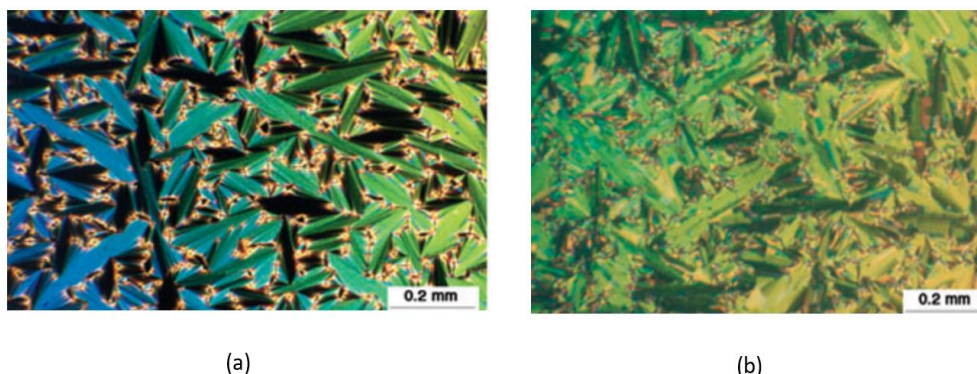


Figure 2.6 The example of smectic mesophase under OPM, (a) SmA (b) SmC (Cuerva et al., 2021b).

Columnar metallomesogens, also known as discotic metallomesogens, have molecule alignments arranged in a 2D crystalline array, stacked together in a column, and have a disk-like shape (Malik et al., 2022). Its molecules are classified based on their packing motives and molecular arrangement within the column, as well as the arrangement of the column itself, which results in a new mesophase. The example columnar mesophase under OPM is shown in Figure 2.7.

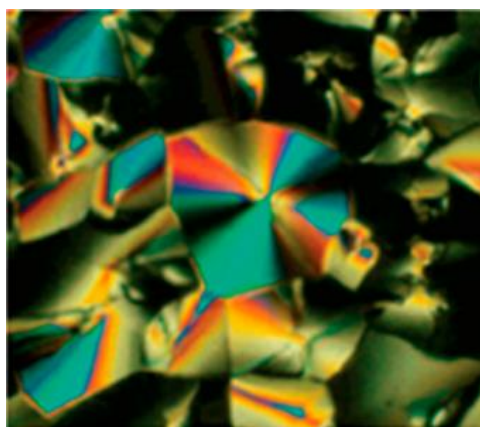


Figure 2.7 Example of columnar mesophase observed under OPM (Cuerva et al., 2021b).

The mesomorphic behaviour of metallomesogen can be studied by using instrument such as Thermogravimetric Analysis (TGA), Differential Scanning Calorimetry (DSC) and Optical polarised microscopy (OPM). The thermal properties of the metallomesogen can be studied using TGA and DSC. TGA investigates thermal stability by analyzing weight changes as temperature increases over time. DSC is a thermal analysis instrument that measures the change in physical properties of a sample with temperature

over time. Besides, since they can easily measure the transition temperatures and transition enthalpies of metallomesogens, these two instruments are well-known and useful techniques for identifying the thermal behaviour of materials (Aswini Krishna et al., 2019). DSC, on the other hand, not only can give information on the transition temperature, but it can also determine the liquid crystalline phases from enthalpy data (Aswini Krishna et al., 2019). As for OPM, this instrument can be used for the study and classification of liquid crystal phases. The optical texture and birefringence of the metallomesogen will be visible under this polarised microscope rather than other regular microscopes because they are polarised and can differentiate the mesophases structure under microscope for nematic, smectic, and columnar.

In addition, the UV-Vis spectroscopy can be used as a qualitative measure in order to determine the geometry structure of metal centre in the metallomesogen complexes. This can be done by measured the highest absorbance value (λ_{max}) *d-d* absorption band of the complexes. The presence of *d-d* absorption bands in a complex can be ascertained through a process that involves calculating the molar absorptivity at the at highest absorbance (ϵ_{max}) using the Beer-Lambert law equation ($A= \epsilon bc$) (Mohammad Isa, 2011). This value is then compared to a benchmark of approximately below $1000 \text{ M}^{-1} \text{ cm}^{-1}$, which is an indicator of the presence of *d-d* bands (Halid, 2016). For Cu(II) complex, the *d-d* absorption band and its highest

absorbance value (λ_{max}) should be observed at about 600 nm for square planar, while 700 nm and 800 nm observed for square pyramidal and octahedral geometry respectively for the Cu(II) metal centre (Aazam et al., 2012; Halid, 2016; Shanmuga Bharathi et al., 2007). As for example, the UV-Vis spectrum that observed a broad *d-d* absorption band at 679 nm with molar absorptivity (ϵ_{max}) of $663 \text{ M}^{-1} \text{ cm}^{-1}$ for the $[\text{Cu}(\text{L}_1)]_2 \cdot \text{H}_2\text{O}$ suggested the square pyramidal for the Cu(II) centre for the complex (Halid, 2016).

2.4 Schiff base ligand

Schiff bases are organic compounds with an imine group ($\text{R}-\text{C}=\text{N}-$) that can be secondary ketamines or secondary aldimines. Schiff bases are also referred to as azomethines. The name Schiff base ligand is taken from the name of the founder, Hugo Schiff, a German chemist who was the first to explain products formed from the reaction of primary amines with carbonyl compounds (Raczuk et al., 2022). The general structure of the Schiff base is shown in Figure 2.8.

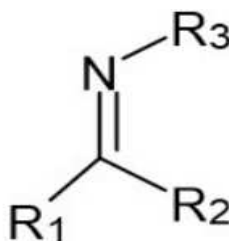


Figure 2.8 The general structure of Schiff base (R_1 =hydrogen, alkyl or aryl, R_2 and R_3 = alkyl or aryl) (Raczuk et al., 2022)

Schiff bases are synthesized through the condensation reaction of a primary amine with a carbonyl group, which can be aldehyde or ketones as shown in Figure 2.9. The reaction is usually under the condition of acid or base catalyst or when heating and it is a reversible reaction. The examples of the Schiff base ligand are as in Figure 2.10.

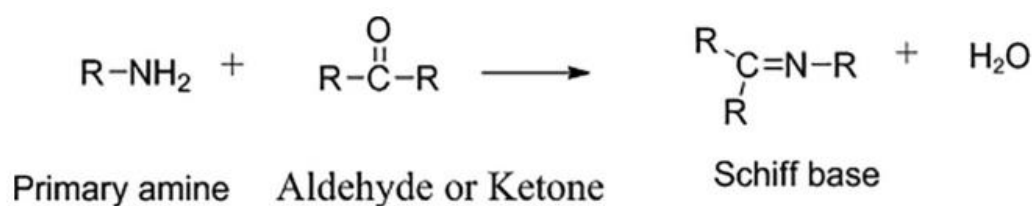


Figure 2.9 The general synthesis of Schiff base ligand (Sadia et al., 2021).

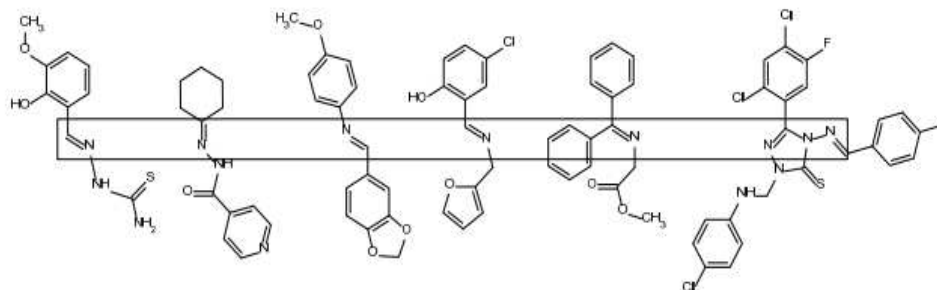


Figure 2.10 Examples of Schiff bases with the imine fragments are framed (Raczuk et al., 2022).

Schiff base ligands have received a lot of attention in the field of coordination chemistry, owing to their ease of synthesis, availability, and electronic properties. Schiff base coordination chemistry has recently received a lot of attention due to its importance in organic synthesis,

analytical chemistry, metal refining, metallurgy, electroplating, and photography. Schiff bases found important use in the dye industry, catalysis, fungicides, and agrochemicals. Several Schiff bases have been reported to have exceptional antibacterial, antifungal, and antiviral and anticancer properties (More et al., 2019). Aside from that, due to their photochromic properties, Schiff base ligands are very suitable compounds to be used as photo stabilizers, solar filters, optical sound recording technology and even dyes for solar collectors. In addition, Schiff base ligand also can have mesomorphic properties, but it varies depending on how rigid and elongated enough the structure is. Just like metallomesogen, mesomorphic properties of Schiff base ligand can be analyzed by using TGA, DSC and OPM.

The structure elucidation of Schiff base ligand can be studied by using $^1\text{H-NMR}$ spectroscopy. This is because $^1\text{H-NMR}$ spectroscopy can be used to determine the content, purity, and molecular structure of a sample, including Schiff base ligand. For example, $^1\text{H-NMR}$ spectra of Schiff base L ligand show a proton at $\delta 15.18$ for NH, a singlet proton at $\delta 9-9.83$ for the $-\text{N} = \text{CH}$ donate the imine moiety and the doublet protons at $\delta 6.83-8.51$ are for naphthalene and pyridine (Sadia et al., 2021). The structure of the Schiff base L ligand is shown in Figure 2.11.

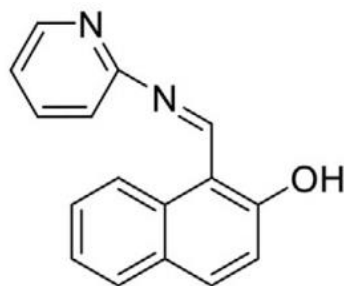


Figure 2.11 Structure of Schiff base Ligand L (Sadia et al., 2021)

Other than $^1\text{H-NMR}$ spectroscopy, Fourier transforms infrared spectroscopy (FTIR) can also be used to determine the structure of a ligand by determining the functional group of a Schiff base ligand. This is because FTIR is a technique for detecting the presence of functional groups in a sample in order to determine or confirm the identity of the pure compound as well as the presence of specific impurities in the sample. Since Schiff base ligands generally have a functional group of imines which is $\text{C}=\text{N}$ stretch, so the strong peak will appear at approximately 1600 cm^{-1} in the spectrum. For example, Schiff base ligand L as shown in Figure 2.11 shows a peak for the functional group of imine ($-\text{C}=\text{N}$) that is found at peaks of 1612 cm^{-1} when the IR analysis of ligand is performed using FTIR spectroscopy at the range of $400\text{-}4000\text{ cm}^{-1}$ (Sadia et al., 2021). From the peak of the spectrum obtained can confirm the synthesized ligand L is for sure a Schiff base ligand as an imine functional group is present in the molecule of the synthesized ligand.

2.5 Schiff base metal complexes

Schiff base ligand can bind with metal to form a metal complex. As for an example of Schiff base ligand combined with transition metal, the ligands (L) with two electron donors that do not undergo electron changes on their valence shells, similar to amines, amides, and phosphines. The complex formation occurs by coordinating the *d*-block metal ion by the electron-donating ligand atom and serves to modify the steric and electronic surroundings of the metal. As a result, the metal ion's reactivity is stabilized and regulated, which is especially useful for less stable ions at higher oxidation states (Raczuk et al., 2022).

Mesomorphism of the metal complex can be affected by the ligand structure. Schiff base ligand coordinates metal ions via azomethine nitrogen, but its lack of strength prevents it from forming stable complexes with metal ions; hence, functional groups such as the hydroxyl group are added as substituents to produce more stable complexes. (Halid, 2016). Schiff bases act as a connecting group between rigid core groups such as benzene and retain molecular linearity, providing greater stability and allowing the formation of mesophases due to the rigidity and flexibility of ligand structure regardless of the fact that it has a stepped core structure (Hagar et al., 2018). This means that, other than combining with a metal ion, Schiff base ligands also can bind with core group which then can induce the

mesomorphism of the ligands as well as their metal complexes. Aside from that, due to the resulting molecular rigidity and flexibility, Schiff base ligand can exhibit mesomorphic behaviour, generating suitable magnitudes of anisotropic end-to-end and lateral intermolecular attractions (Nakum et al., 2020). The study on N-(4-((4-n-Alkoxy-2-hydroxybenzylidene)amino)phenyl) acetamide Schiff base ligand with different number of carbons on alkoxy terminal end group shows mesomorphic behavior of ligand starting from hexyloxy ($-\text{OC}_6\text{H}_{13}$) to octyloxy ($-\text{OC}_8\text{H}_{17}$) terminal end group while its Cu(II) complexes show mesomorphism starting from octyloxy ($-\text{OC}_8\text{H}_{17}$) to n-octadecyloxy ($-\text{OC}_{18}\text{H}_{31}$) (Nakum et al., 2020). This shows that increasing the carbon chain of the alkoxy terminal end group length at certain point will increase the likelihood of mesomorphism or mesomorphic properties.

Schiff bases and their complexes are very interesting topic to be studied as Schiff bases and their complexes have numerous applications in catalysis, synthesis, polymerization, epoxidation of olefins, dye degradation via decomposition of hydrogen peroxide and other reagents, textile industries, biological, as well as photochromic applications (Dehghani Firuzabadi et al., 2018). Schiff bases and their metal complexes are often used as analgesics, anti-inflammatory, analgesics, anticancer, antiviral, fungicidal, pesticidal, bactericidal, insecticidal, herbicidal, and growth regulators. It also reported that ligand containing metal have high antibacterial activity in

compare to free ligands (More et al., 2019). Not just that, they were used in the manufacture of high temperature and automobile antiglare mirrors, organic semiconductors, filaments, deodorants, light stabilizers, dental materials, cross-linked polymers, corrosion inhibitors, and perfumes. Many scientists have been fascinated by the synthesis, structure, and properties of Schiff base complexes over the last couple of decades to their significant contributions to single molecule-based magnetism, material science, and catalysis of several reactions, including carbonylation, hydroformylation, reduction, oxidation, epoxidation, and hydrolysis, and many others. Furthermore, many Schiff base complexes demonstrated excellent catalytic activity in a variety of reactions at elevated temperatures ($>100^{\circ}\text{C}$) and in the presence of moisture. Due to its exciting properties with their complexes, a substantial amount of research has been published on the synthesis, structural investigations, various crystallographic features, mesogenic properties, structure-redox relationships, and catalytic properties of various types of Schiff base ligands and their complexes with transition and non-transition elements (Jadhav & Kapadnis, 2018).

2.5.1 Copper (II) Schiff base metal complexes

Copper (Cu) is a reddish-brown transition metal element (*d*-block) that located in the first row of the periodic table, where transition metals from this row are well known for being cheaper, very easy to handle, readily

available in pure state, and simple to analyze. This metal has electronic configuration of $3d^{10}4s^1$. Aside from that Cu has three major oxidation states which are zero (pure metal), +1 ous-suffix added compounds, and +2 ic-suffix added compounds (Mustafa & AlSharif, 2018). This metal can forms complexes with appropriate ions and radicals and found in various complexes in the d^9 -state (Mustafa & AlSharif, 2018).

Both ligands and metal ions can influence the thermal stability and melting point of the metallomesogen. As for ligand, to design the metal complex with increased thermal stability, either stimulate self-assembly via-H bond formation or decrease melting point by reducing molecular symmetry and using the ligands with long or non-linear alkyl chains can be used as an alternative (Mat & Mohamadin, 2020). When it comes to metal ions, choosing a metal that is thermally stable and has a lower melting point, such as copper metal, is a key solution. Generally, transition metals have unique properties in terms of electronic conductivity, thermal stability, colour, and magnetic properties, whereas for Cu, it has high thermal stability and electrical conductivity which as a result of these unique properties, it has become one of the most important metals and is widely used in research (Ozair et al., 2019). In addition to that, research has demonstrated that the inclusion of Cu metal in Schiff base complexes contributes to the stabilization of the mesophase at higher temperatures (Nakum et al., 2020).

Because of these properties, Schiff base Cu(II) complexes have potential applications as semiconductors and optoelectronic devices.

Cu is a metal that is special in many ways, and when combined with other elements to form a complex, it can have several benefits. One of the most exciting potential uses for copper complexes is in the development of anti-cancer compounds, which have the ability to kill cancer cells in a variety of ways, including by inhibiting proteosomes, creating reactive oxygen species, and damaging DNA (Yusuf et al., 2021). Copper complexes have an advantage over other types of therapeutic agents, as they are typically more soluble, making them easier to use in medical applications. Recently, there has been a resurgence of interest in copper-based complexes, with researchers working to develop new compounds that could be used for a wide range of medical purposes. This research could have important implications for the future of medicine, and lead to the development of more effective treatments for a variety of diseases. For example, Cu(II)indomethacin complexes have been used in veterinary medicine as an anti-inflammatory medicine (Yusuf et al., 2021).

Aside from that, researchers are investigating the use of metal complexes like Cu to develop efficient and cost-effective optoelectronic devices. These devices can perform both electronic and light functions and are currently

used in various fields like medicine, information technology, and the military (Ozair et al., 2019). Copper complexes are considered a promising material for use in these devices due to their potential to provide significant functions. To improve device efficiency, suitable materials and complexes are needed, and Cu complexes are one of the options being explored (Ozair et al., 2019). In addition, Cu(II) complexes are also thought to have a low melting point, in contrast to the majority of metallomesogens, which have high melting points that are greater than 523 K (Ozair et al., 2019). As for Schiff base Cu(II) complexes and other transition metal Schiff base complexes such as zinc, and cadmium, have been shown to be excellent precursors for the synthesis of metal or metal chalcogenide nanoparticles (More et al., 2019) and they also known to be very vital in antibacterial properties. Due to these unique properties of Cu(II) complexes and Cu(II) Schiff base complexes, many researchers from various fields are attracted to study them.

Cu(II) Schiff base complexes can be synthesized by reacting Schiff base ligands with either Cu(II) acetate monohydrate or Cu(II) salt. As for example, the synthesis of Cu(II) complexes with its Schiff base homologous series ligands which is on N-(4-((4-n-Alkoxy-2-hydroxybenzylidene)amino)phenyl)acetamide were prepared by dissolving (2 mmol) of Cu(II) acetate monohydrate in a minimal amount of ethanol, and the solution then being added to a hot ethanolic solution of ligand (n=2–8, 10, 12, 14, 16, 18,

4 mmol). The mixture refluxed for 4 hours. A crystalline solid formed were then filtered, washed with hot distilled water and then ethanol, and dried under vacuum (Nakum et al., 2020).

FTIR spectroscopy can be used to analyze Cu(II) Schiff base complexes in order to confirm their structure by confirming the presence of functional groups in the structure. The IR spectrum of Cu(II) complexes with their Schiff base homologous series ligands, N-(4-((4-n-Alkoxy-2-hydroxybenzylidene)amino)phenyl)acetamide (series A), for example, showed peaks for carbonyl stretching at around 1657–1658 cm^{-1} for metal complexes and 1661 cm^{-1} for ligands (series-A). Metal complexes and ligand (series A) show bands for (C=N) at 16011–1609 cm^{-1} and 1627–1621 cm^{-1} , respectively, where the lower peak in metal complexes indicates complex formation via N of the azomethine group. Peaks in the spectrum are also seen around 591–589 cm^{-1} and 542–537 cm^{-1} due to (M–N) and (M–O) vibrations (Nakum et al., 2020).

CHAPTER 3

METHODOLOGY

3.1 Materials

2,4-dihydroxybenzaldehyde

Potassium bicarbonate (KHCO_3)

Potassium iodide (KI)

1-bromodecane

HCl

Distilled water

Chloroform

Ethylenediamine

Acetic acid

Ethanol

Cu(II) acetate monohydrate

3.2 Apparatus

Spatula

Beaker, 200 mL

Measuring cylinder, 10 mL, 200 mL

Analytical balance

Reflux set

Suction flask

Suction pump

Retort stand

Glass rod

Filter paper

Funnel

Dropper

Vials

Stickers

3.3 Instrumentation

FTIR-Spectroscopy

Nuclear Magnetic Resonance, NMR

UV-Vis spectroscopy

Magnetic Susceptibility

Thermogravimetric analyser, TGA

Differential scanning calorimetry, DSC

Optical polarised microscope, OPM

3.4 Methods

3.4.1 Synthesis of Schiff base ligand (H₂L)

5 mmol (0.7 g) 2,4-Dihydroxybenzaldehyde, 2.5 mmol (0.2 ml) ethylenediamine and a few drops of acetic acid as a catalyst were added to 20 ml of ethanol. The mixture was refluxed for 1 hour at temperature of 70°C and the yellow Schiff base ligand (H₂L) was obtained. Then, the compound was collected by filtration, recrystallized using ethanol and dried with suction pump (Pramanik et al., 2016).

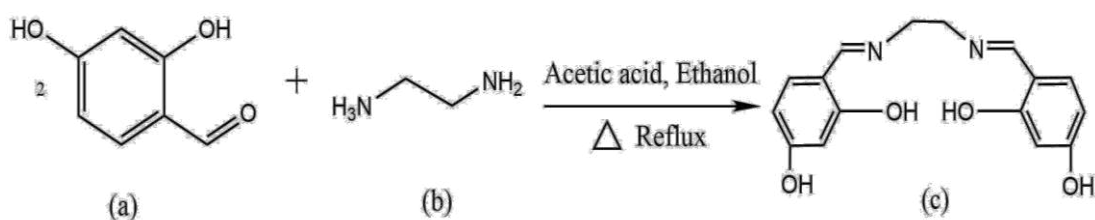


Figure 3.1 Structural formula of (a) 2,4-dihydroxybenzaldehyde, (b) ethylenediamine, (c) Schiff base ligand (H₂L)

3.4.2 Synthesis of Copper (II) Complex (CuL)

2 mmol (0.6 g) H₂L was placed into the round bottom flask with 20 ml of ethanol. 4 mmol (0.799 g) copper (II) acetate monohydrate was added to 10 ml of ethanol solution. The mixture was dissolved in a small amount of hot ethanol. Then the mixture was added portion wise into the Schiff base ligand mixture while heating and refluxed for 3 hours. The purple precipitate was

collected by filtration, wash with cold ethanol and dried with suction pump (Guo et al., 2019).

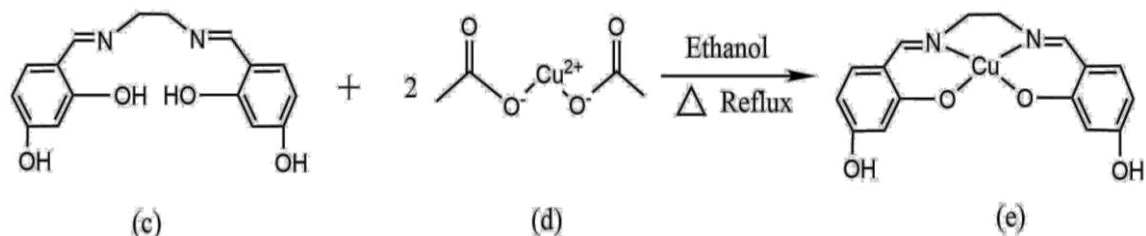


Figure 3. 2 Synthesis of Cu (II) complex (CuL), the structure (c) Schiff base ligand (H₂L) (d) Copper (II) Acetate monohydrate and (e) proposed structure of Cu (II) complex (CuL)

3.4.3 Synthesis of elongated Copper (II) Complexes (CuLC₁₀)

1.66 mmol (0.6 g) of CuL complex, and 3.32 mmol (0.69 ml) 1-bromodecane were mixed into the 20 ml of ethanol (Derkach et al., 2014). The mixture was heated under reflux and stirred at the temperature of 70°C for 4 hours. The mixture was left to cool at room temperature. The purple precipitate was collected by filtration, wash with cold ethanol and dried with suction pump (Pramanik et al., 2016).

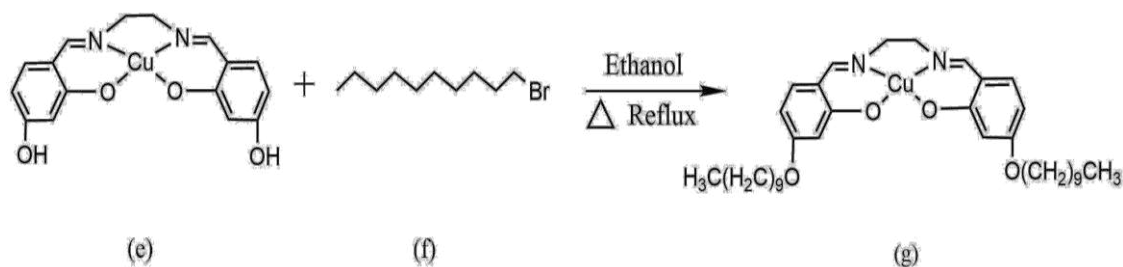


Figure 3.3 Synthesis of elongated Cu(II) complex (CuLC₁₀) and structure of (e) proposed structure of Cu (II) complex (CuL), (f) 1-bromodecane and proposed structure of (g) elongated Copper (II) complex (CuLC₁₀)

3.5.1 Instrumental Analysis

3.5.1 Nuclear magnetic resonance (NMR)

The Schiff base ligand (H₂L) sample was analyzed using NMR. The NMR spectra was recorded using Bruker AV400III HD 400MHz (¹H 400 MHz) model and DMSO-d₆ was used as a solvent. The chemical shift used as a reference to the residual DMSO-d₆ in the deuterated solvent.

3.5.2 FTIR-spectroscopy

Both Schiff base ligand (H₂L) and Cu(II) Schiff base complexes (CuL and CuLC₁₀) that synthesized was analyzed using FTIR. The sample was placed on the ATR pellet and recorded on a Perkin Elmer Frontier model where the pellet was mount on the holder. The spectrum was recorded in the range of 4000-600 cm⁻¹. The peaks were assigned by comparing it with the

corresponding wavenumber from the literature. The step then will be repeated by using Cu(II) Schiff base complex sample (CuL and CuLC₁₀) and results analysis of both samples will be compared.

3.5.3 UV-Vis-spectroscopy

Both Cu(II) Schiff base complexes (CuL and CuLC₁₀) that synthesized were analyzed using UV-Vis spectroscopy. Both solid samples were first dissolved using DMSO. The UV-Vis spectra were recorded on a Evolution 201/220 UV-Visible Spectrophotometers model. The spectrum was recorded in 1-cm quartz cuvettes in the range of 1000-400 nm.

3.5.4 Magnetic susceptibility

At room temperature, a Sherwood Scientific magnetic susceptibility balance was utilized to measure the magnetic moment. The material was crushed with a dry agate pestle and mortar that was kept clean. The mass susceptibility of the complex was measured after a little amount of the substance was packed to the mark inside a short cylindrical tube. The analysis using magnetic susceptibility was conducted in the University Malaya laboratory.

3.5.5 Thermogravimetric analysis (TGA)

Cu(II) Schiff base complex (CuL) that was synthesized was analyzed by using TGA for thermal stability properties. The TGA analysis was done by using the Pyris Diamond TG/DTA Perkin Elmer Thermogravimetric Analyzer TGA6 model with scan rate of $20^{\circ}\text{C min}^{-1}$ under N_2 (Farhan et al., 2015). A 4-7 mg of Cu(II) Schiff base complex powder was introduced into alumina crucible before inserted into the sample holder and then was heated under nitrogen purge in range of 50°C to 900°C .

3.5.6 Differential scanning calorimetry (DSC)

Cu(II) Schiff base complex (CuLC_{10}) that are synthesized was analyzed by using DSC. The DSC thermograph was obtained using a Mettler Toledo DSC 822 model with a scan rate of $5^{\circ}\text{C min}^{-1}$. About 0.6 to 0.8 mg of Cu(II) Schiff base complex powder were introduced into the aluminium crucible and was heated in the sample holder for the first heating cycle from 60°C to 180°C . The procedure was followed by a cooling cycle from 180°C to 60°C and finally back to the second heating cycle, which is 180°C . The analysis using DSC was conducted in the University Malaya lab.

3.5.7 Optical polarised microscopy (OPM)

The liquid crystal phase of Cu(II) complex (CuLC₁₀) was observed under optical polarised microscopy (OPM) of Olympus polarising microscope model that was equipped with a Mettler Toledo FP90 central processor and FN82HT hot stage. The small amount of Cu(II) Schiff base complex (CuLC₁₀) sample was placed onto a clean glass slide which will then was placed onto the hot stage. The heating and cooling rates were adjusted between 2-5°C min⁻¹ that was depending on the sample's suitability. The magnification was adjusted to 80x. The analysis using OPM was conducted in the University Malaya lab.

CHAPTER 4

RESULTS AND DISCUSSIONS

4.1 Introduction

In order to accomplish the primary goal of this research project, which was to synthesize and analyze a Copper (II) complex as a prospective metallomesogens, a Schiff base ligand was reacted with Copper(II) acetate to produce a novel complex, and then the complex structure was further subjected to characterization by using various instrumental analysis.

The structural formulas of the ligand and complex were deduced from the result of Fourier Transform Infrared spectroscopy (FTIR) and $^1\text{H-NMR}$ spectroscopies. As for the geometry of the Cu(II) metal centre, both complexes (CuL and CuLC₁₀) were determined by using UV-Vis spectroscopy. The magnetic properties of the final complex, CuLC₁₀ was determined by using magnetic susceptibility instrument analysis that was measured by Gouy method. The thermal properties of the complex was obtained from thermogravimetry analysis (TGA) and the mesomorphic characteristics were observed by using differential scanning calorimetry (DSC) and optical polarised microscope (OPM).

4.2 Structure elucidation of H₂L Schiff base ligand

H₂L Schiff base ligand was obtained through the reaction of 2,4-dihydroxybenzaldehyde with ethylenediamine in ethanol as solution and yellow solid was obtained and the percentage yield was 89.8%. The structural formula for the free Schiff base ligand (H₂L) was proposed from combined result of FTIR and ¹H-NMR spectroscopies.

The FTIR spectrum of the free ligand, which is H₂L ligand in Figure 4.1 shows the strong characteristic bands of the (C=N)_{imine} functional groups at 1638 cm⁻¹. The (O-H) stretching frequency of this free ligand is expected to appear at around 3500 to 2500 cm⁻¹. Because of the presence of a strong intramolecular hydrogen bond between (O-H) and (C=N) bonds, there is no O-H peak recorded at this range. This is because the O-H band has shifted to lower frequencies, which can be found in the region of 3200 to 2500 cm⁻¹ (Bartyzel, 2017). The fact that the spectra shows, the (O-H) band emerges as broad bands at 2555 cm⁻¹ is further an indication that a significant hydrogen bond exists between the hydroxyl group (O-H) and the azomethine group (C=N). The presence of an in-plane bending (O-H) vibration is confirmed by the medium peak that appears at 1355 cm⁻¹. In the spectrum also can be observed very strong stretching band at 1231 cm⁻¹ which assigned for (C-O) stretching for phenol group. The FTIR spectrum also shows two peaks at 2971 cm⁻¹ and 2867 cm⁻¹ for asymmetric and

symmetric (C-H) stretching respectively, indicating the existence of two (CH₂) for the ligand spacer.

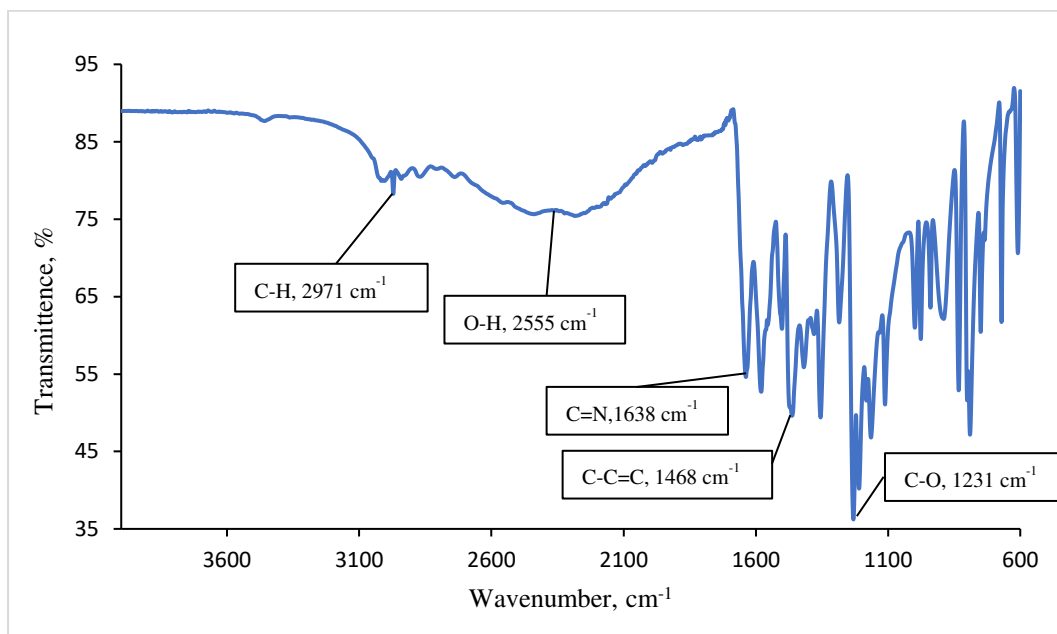


Figure 4. 1 FTIR spectra for free ligand H₂L

Figure 4.2 displays ¹H-NMR spectra of the H₂L ligand that were recorded at 298 K in DMSO d₆. Broad signals measured at 13.66 and 9.67 ppm are easily explained by the presence of phenolic OH-A and OH-B moieties, respectively. The aromatic protons of the salen ligand resonated in the range of 6.16–7.17 ppm, and they were precisely identified according to their J coupling constants, which were found to be at 7.16, 6.26, and 3.78 ppm for H-D, H-E, and H-F, respectively. At a signal of 8.36 ppm, the proton singlet that was predicted to be present in the imine moiety (H-C) was found.

Additionally, a singlet of the aliphatic protons (H-G) was recorded with a signal of 3.78 ppm.

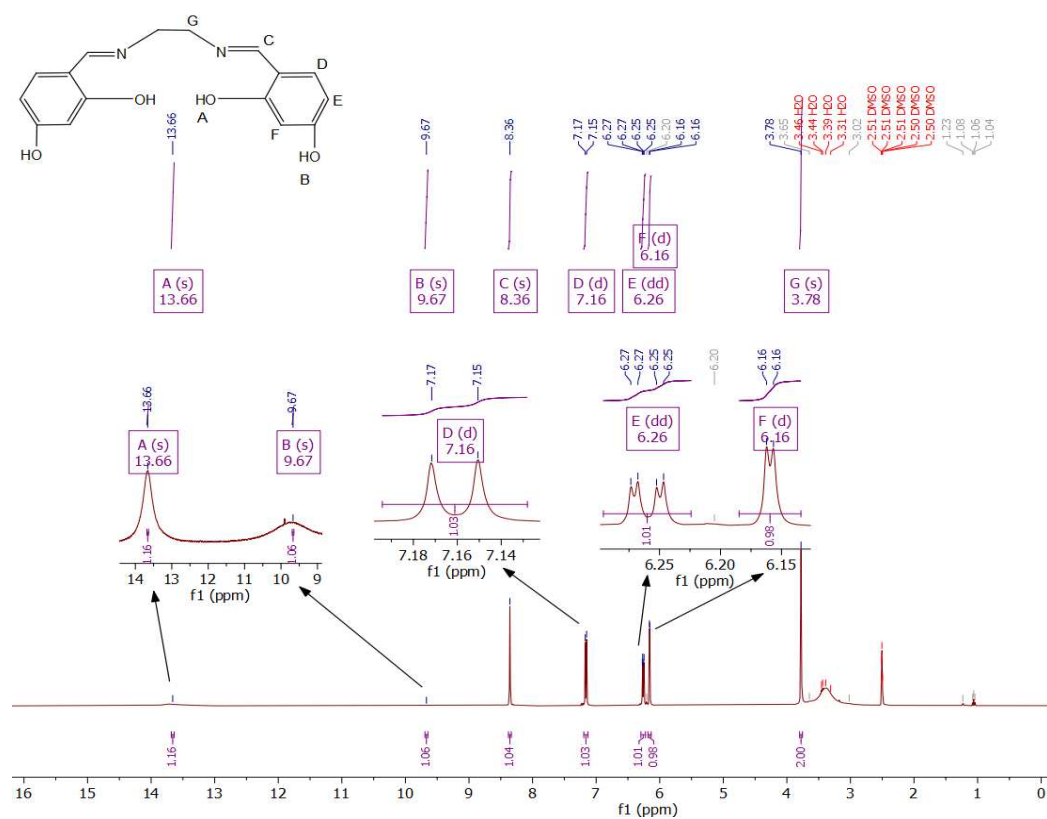


Figure 4. 2 ^1H -NMR spectra for free Schiff base ligand H_2L

Table 4. 1 The ^1H -NMR data and peak assignments for free Schiff base ligand, H_2L

Chemical Shift (ppm)	Range	Integral ratio	H's	Multiplicity	Assignment
3.78	3.80 - 3.75	2.00	2	singlet	H-G
6.16	6.18 - 6.13	0.98	1	doublet	H-F
6.26	6.30 - 6.22	1.01	1	doublet of doublet	H-E
7.16	7.19 - 7.13	1.03	1	doublet	H-D
8.36	8.38 - 8.33	1.04	1	singlet	H-C
9.67	9.69 - 9.65	1.06	1	singlet	H-B
13.66	13.68 - 13.64	1.16	1	singlet	H-A

Based on both the FTIR and $^1\text{H-NMR}$ spectra, the proposed structure for H_2L is as Figure 4.3 with the molecular formula of $\text{C}_{16}\text{H}_{16}\text{N}_2\text{O}_4$.

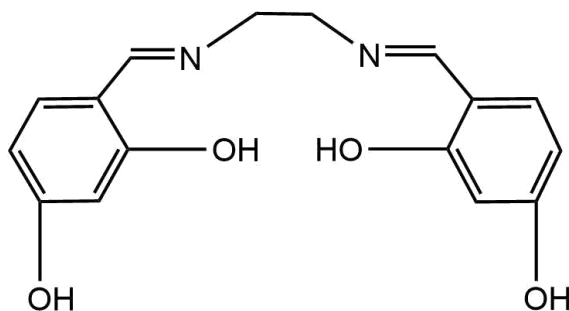


Figure 4.3 Proposed structure for free Schiff base ligand H_2L

4.3 Structure elucidation of CuL

CuL complex was obtained through the reaction of H_2L ligand with Cu(II) Acetate in ethanol as a solution for the reaction and purple solid was obtained. The percentage yield for the product obtained was 96.7%. The suggested structural formula was obtained from combined result of FTIR spectroscopy and the UV-Vis spectroscopy.

In the FTIR spectra for the CuL complex in Figure 4.4 shows the strong stretching peak of the $(\text{C}=\text{N})$ at 1604 cm^{-1} which shifted to lower wavelength in compare to free ligand H_2L shows there is coordination of azomethine group with Cu(II) metal. The wavelength of $(\text{C}=\text{N})$ group that shifted to lower frequency after the complexation of Cu(II) indicated there was the

coordination between the azomethine group (C=N) with the Cu(II) metal (Hosseinzadeh Sanatkar et al., 2020). As for the (O-H) for phenolic group, a broad band peak of the (O-H) moieties can be observed at 3442 cm^{-1} which is shifted toward higher wavelength in compared to free ligand H_2L . This indicate that there is no more strong intramolecular hydrogen bond between (O-H) and (C=N) bonds but instead indicating the coordination of coordination of (C=N) with Cu(II) ion (Bartyzel, 2017). In addition, the vibration peak of (C-O) group was shifted to lower frequencies in compare to the free ligand where it is observed at 1221 cm^{-1} , in which further confirms the complexation of metal centre Cu(II). Moreover, the FTIR spectrum of CuL showed the (Cu-O) at 620 cm^{-1} .

The medium asymmetric and symmetric (C-H) peaks for CH_2 were both found at 2971 cm^{-1} and 2867 cm^{-1} in the FTIR spectrum for the ligand spacer. The acetate ions peaks also can be observed in the spectra for both deprotonated carboxylic group of acetate asymmetric and symmetric stretching of COO at 1541 cm^{-1} and 1448 cm^{-1} respectively. The Δ value of both COO peaks was 93 cm^{-1} that is indicate the chelating binding mode for the acetate ion CH_3COO^- which is almost similar reported for complex $[\text{Ni}_2(\text{CH}_3\text{COO})_2(\text{L1})].3\text{H}_2\text{O}$ that have Δ value of 98 cm^{-1} for chelating binding mode for acetate ion (Halid, 2016).

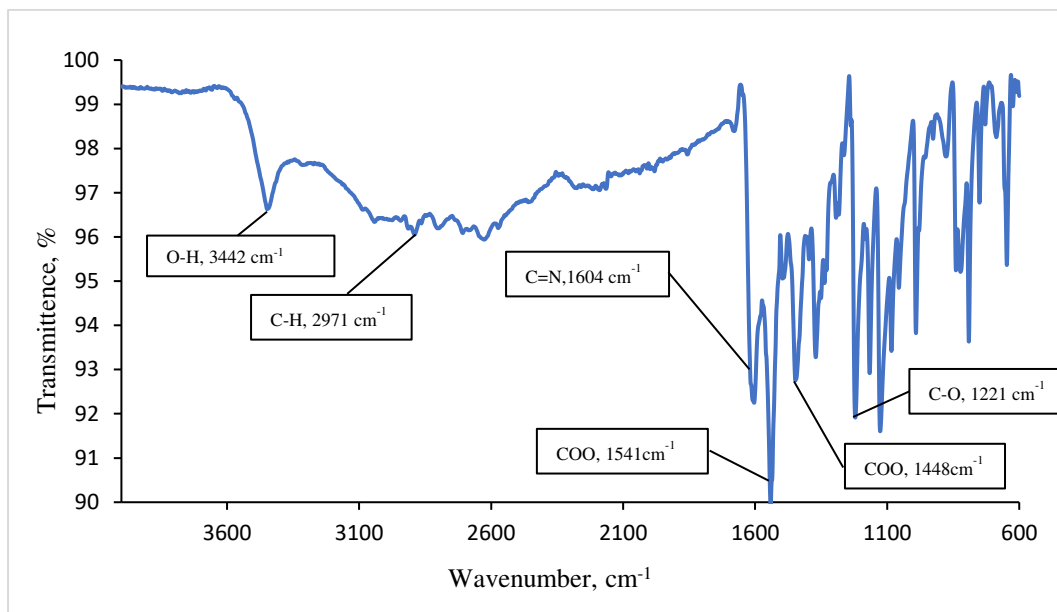


Figure 4.4 FTIR spectra for CuL complex

The UV-Vis spectrum in Figure 4.5 was recorded in DMSO. The spectrum shows a broad *d-d* absorption band at 610 nm with molar absorptivity (ϵ_{max}) of $663 \text{ M}^{-1} \text{ cm}^{-1}$ suggest a square planar for Cu(II) centre in the CuL complex. This is because the molar absorptivity (ϵ_{max}) for the highest absorbance (λ_{max}) is roughly below $1000 \text{ M}^{-1} \text{ cm}^{-1}$ allocated for the *d-d* band, while the highest absorbance at the respective *d-d* band with a value of about 600 nm should be showing square planar structures (Shanmuga Bharathi et al., 2007)

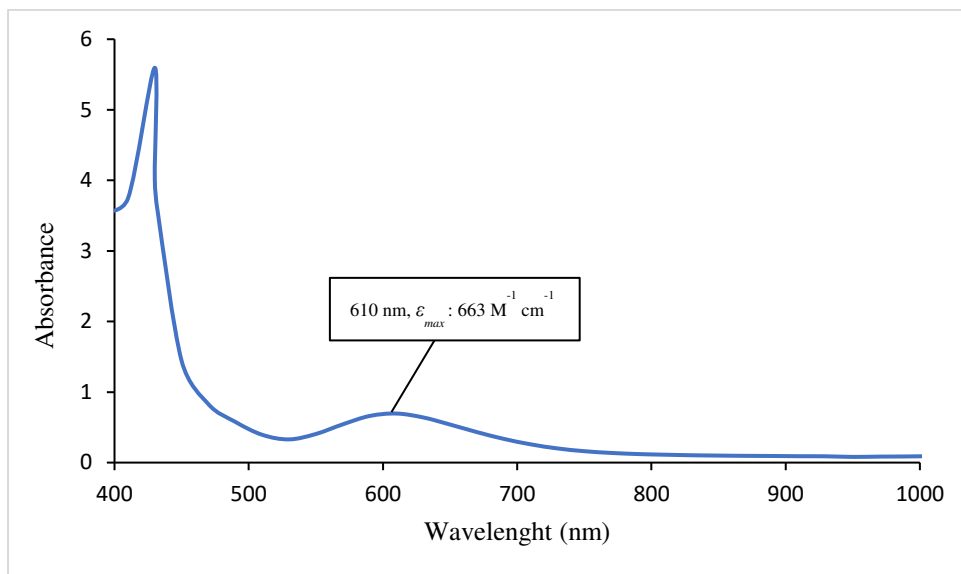


Figure 4.5 UV-Vis spectra for CuL complex

Based on combined both data from the FTIR and UV-Vis spectroscopy, the proposed structure for CuL complex is as Figure 4.6 with the molecular formula of $\text{C}_{20}\text{H}_{20}\text{Cu}_2\text{N}_2\text{O}_8$.

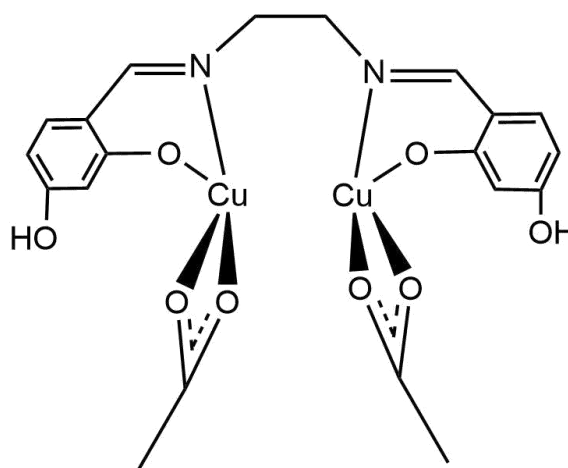


Figure 4.6 Proposed structure for CuL complex

4.4 Structure elucidation of CuLC₁₀

The CuLC₁₀ complex was obtained through the reaction of CuL with 1-bromodecane in ethanol as solution and purple solid was obtained as the product. The percentage yield for the product obtained through the reaction was 50.5%. The suggested structural formula was concluded from combined result of FTIR spectroscopy, UV-Vis spectroscopy, TGA and magnetic susceptibility. The mesomorphism of the complex was studied using DSC and OPM.

In the FTIR spectra for the CuLC₁₀ in Figure 4.7 also shows the strong stretching peak of the (C=N) at 1614 cm⁻¹ which shifted to lower wavelength in compare to free ligand H₂L in which also shows there is coordination of azomethine group with Cu(II) metal (Hosseinzadeh Sanatkar et al., 2020). As for the (O-H) for phenolic group similar with the CuL complex, a broad band peak of the (O-H) moieties can be observed at 3447 cm⁻¹ which is shifted toward higher wavelength in compare to free ligand H₂L which indicate no more strong intramolecular hydrogen bond between (O-H) and (C=N) bonds but instead the coordination of (C=N) with Cu(II) ion (Bartyzel, 2017). Similar to CuL complex the vibration peak of phenol (C-O) group was shifted to lower frequencies in compare to the free ligand and observed at 1221 cm⁻¹, confirms the complexation of metal centre Cu(II) with (C-O). The medium asymmetric and symmetric (C-H) peaks for CH₂

of ligand spacer were both found at 2923 cm^{-1} and 2853 cm^{-1} in the FTIR spectrum which also almost similar to CuL complex. The acetate ions peaks also can be observed in the spectra for both deprotonated carboxylic group of acetate asymmetric and symmetric stretching of COO at 1541 cm^{-1} and 1449 cm^{-1} respectively with the Δ value of 92 cm^{-1} that is also indicate the chelating binding mode for the acetate ion CH_3COO^- which is similar to the CuL complex.

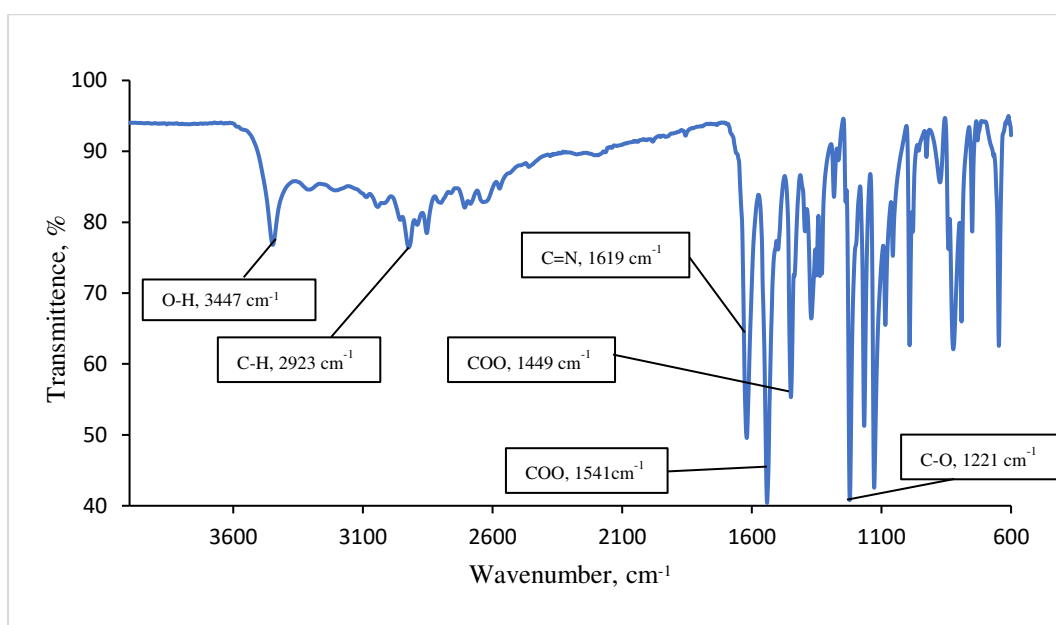


Figure 4.7 FTIR spectra for CuLC₁₀ complex

The UV-Vis spectrum in Figure 4.8 was recorded in DMSO. Similar with CuL complex, the spectrum shows a broad *d-d* absorption band at 610 nm with molar absorptivity (ϵ_{max}) of $663\text{ M}^{-1}\text{ cm}^{-1}$ which suggest a square planar for Cu(II) centre in the CuLC₁₀ complex.

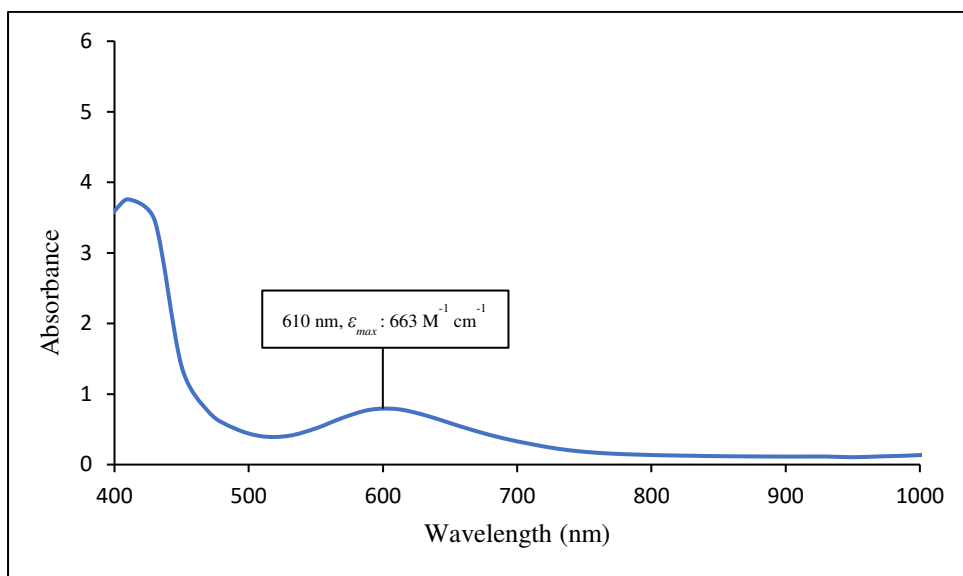


Figure 4. 8 UV-Vis spectra for CuLC₁₀ complex

(a) Magnetic Properties

The effective magnetic moment (μ_{eff}) calculated was 3.005 BM at 298 K. the value was calculated using the formula of $\mu_{\text{eff}} = 2.83[T(\chi_{\text{m}}^{\text{corr}} - N\alpha)]^{1/2}$ with the following data: $\chi_{\text{g}} = 0.676 \times 10^{-6} \text{ cm}^3 \text{ g}^{-1}$, $\chi_{\text{m}} = 3.67 \times 10^{-3} \text{ cm}^3 \text{ mol}^{-1}$, $\chi_{\text{dia}} = -1.09 \times 10^{-4} \text{ cm}^3 \text{ mol}^{-1}$, $\chi_{\text{m}}^{\text{corr}} = 3.78 \times 10^{-3} \text{ cm}^3 \text{ mol}^{-1}$ (de Berg & Chapman, 2001). The calculated value is quite higher than the expected spin-only value calculated which is 2.83 BM for two Cu(II) centres. However, it is still in good agreement with dinuclear Cu(II) complex (2 unpaired electrons). This indicates that the CuLC₁₀ complex is paramagnetic and a dinuclear complex which contains two Cu(II) metal centres.

(b) Thermal Properties

The TGA trace in Figure 4.9 shows an initial weight loss of 16.15% from about 64°C to 339°C which is expected due to the evaporation of two acetate ions (CH_3COO^-). The initial weight loss of 16.15% are quite low in compared to calculated value which is 21.7% but it is still in a good agreement. The second weight loss of 54.09% from 339°C to 679°C is assigned to the decomposition of the ligand (L) (calculated 54.9%). As for amount of residue at temperature above 679°C which was 29.07% (calculated 29.2%) was assumed to be the decomposition of pure two CuO molecules. From this TGA analysis, identified that the CuLC_{10} complex was thermally stable up to 64°C and started decomposed for temperature higher than 64°C. From the decomposition of the ligand and whole complex by comparing to calculation value and TGA data, the CuLC_{10} complex might not be coordinated with the long alkyl chain, C_{10} (long terminal end alkoxy group) from the synthesis with 1-bromodecane. Besides, this TGA analysis also further confirmed the presence of coordination of CuLC_{10} complex with two Cu(II) metal as metal centres.

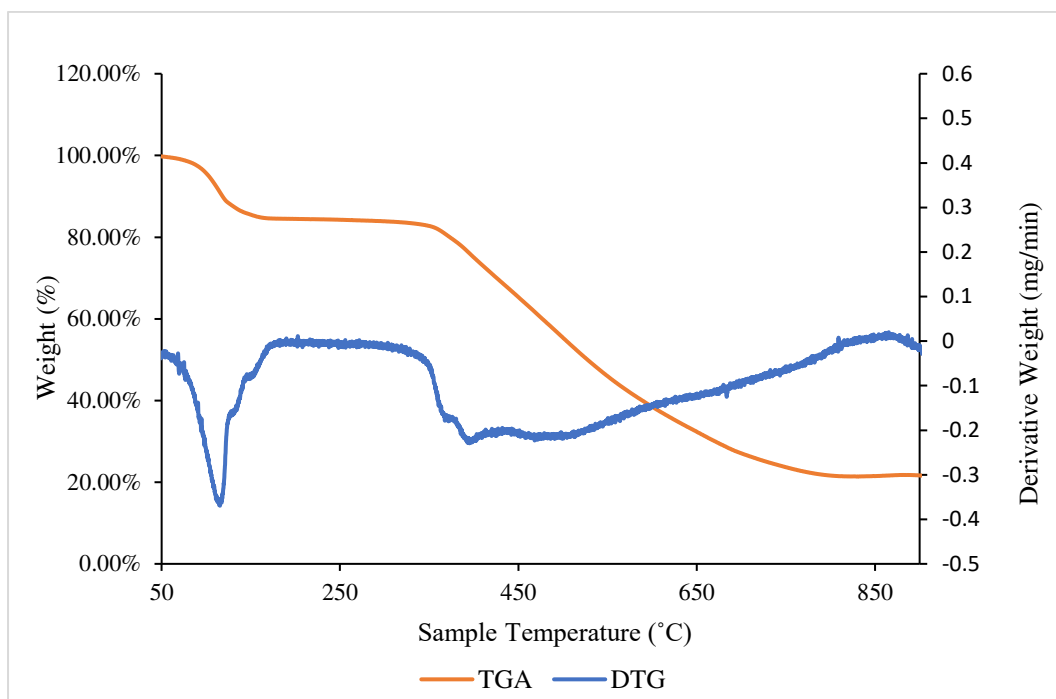


Figure 4. 9 TGA of CuLC₁₀ complex

(c) Mesomorphic Properties

The DSC spectrum in Figure 4.10 was recorded for the heating and cooling cycle that was recorded from 60°C to 180°C. There was recorded an endothermic peak upon heating from 152.0°C to 165.3°C ($\Delta H = 50.57 \text{ kJ mol}^{-1}$) where it is assigned as melting temperature for CuLC₁₀ complex. However, there was no peak recorded upon cooling of the complex. From the DSC data, there was no indication of liquid crystalline phases from enthalpy data.

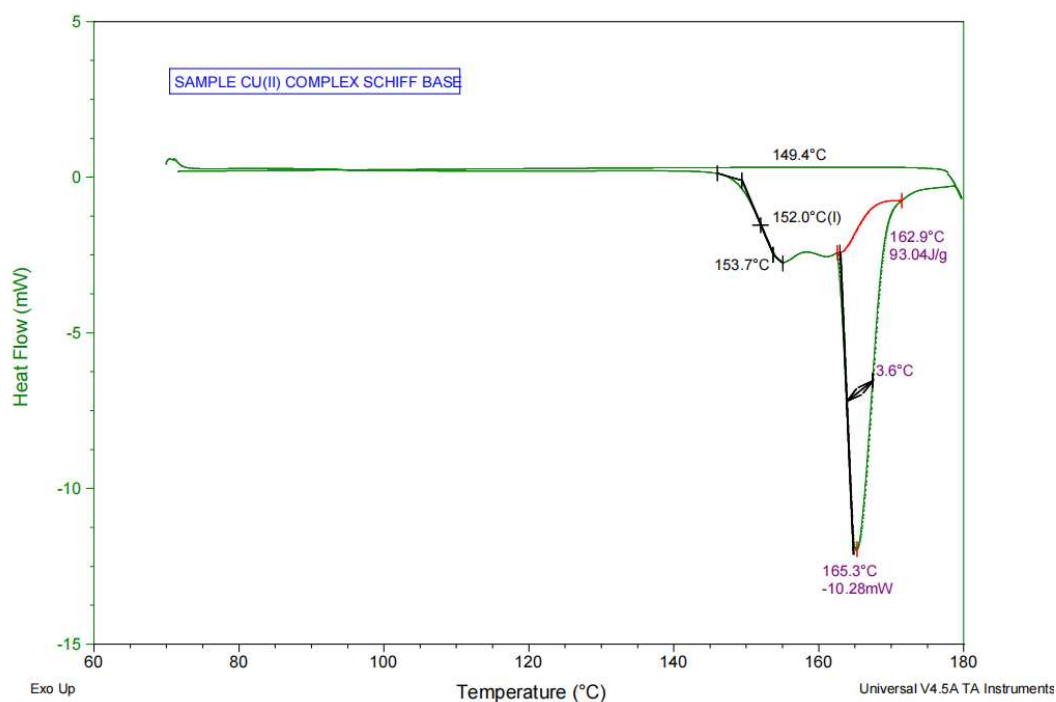


Figure 4. 10 DSC of CuLC₁₀ complex

CuLC₁₀ complex viewed under Optical Polarized Microscope (OPM) in Figure 4.11 showed no mesomorphism optical textures or birefringence for CuLC₁₀ complex. Based on both the DSC and OPM results, the CuLC₁₀ complex was melting on heating at 150°C. This can be shown in Figure 4.12 that shows the small changes in the optical texture of the CuLC₁₀ complex upon heating above 150°C due to melting. From both DSC and OPM analysis can be concluded that the CuLC₁₀ complex does not exhibit any mesomorphism behaviour.

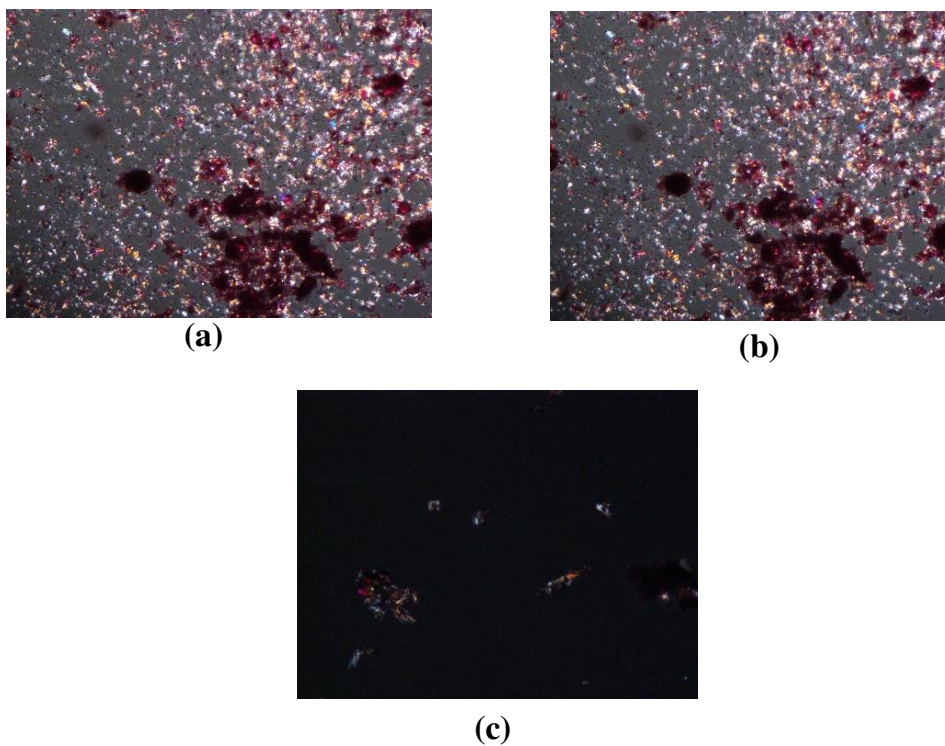


Figure 4. 11 Photomicrographs for CuLC₁₀ complex on: (a) heating at room temperature at 30°C; (b) heating at 60°C and (c) heating at 86°C with 50x magnification.

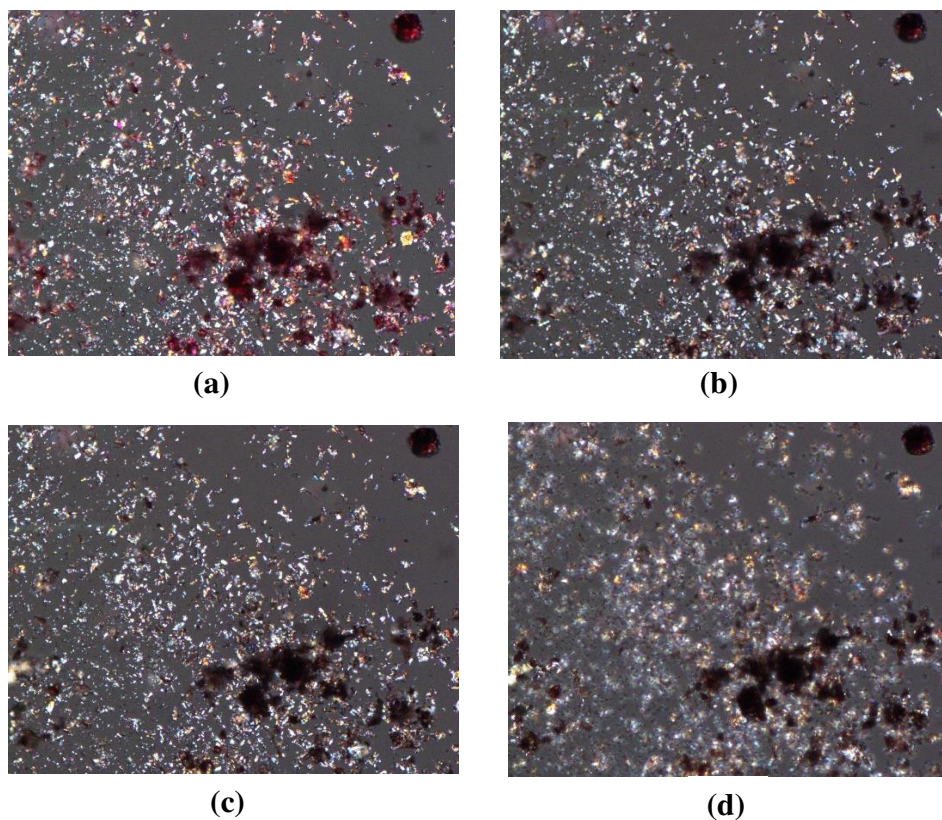


Figure 4. 12 Photomicrographs for CuLC₁₀ complex on: (a) heating at room temperature at 100°C; (b) heating at 150°C; (c) heating at 180°C. and (d) heating at 200°C.

Combining all the results for CuLC₁₀, the suggested structure for the complex is as Figure 4.13 with a molecular formula of C₂₀H₂₀Cu₂N₂O₈. The structure is a dinuclear complex with two Cu(II) metals as centres and does not coordinated with long alkyl chain (alkoxy group) of decane (C₁₀) that may be a reason why the complex did not exhibit the mesomorphism behaviour. The unsuccessful synthesis of CuLC₁₀ complex may be due to unsuitable solvent (ethanol) used for the reaction. Ethanol was used instead of other preferred solvents such as DMF or DMSO in the synthesis reaction

of the complex because the unavailability of DMF and limited amount of DMSO in the laboratory.

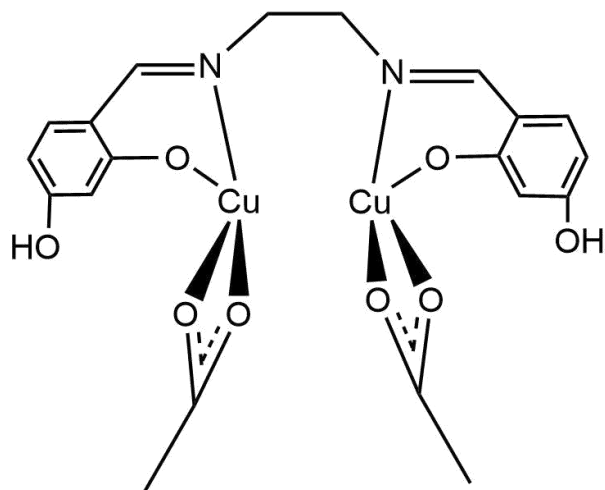


Figure 4. 13 The suggested structure for CuLC₁₀ complex

CHAPTER 5

CONCLUSION AND RECOMMENDATIONS

5.1 Conclusion

In this study, a range of techniques was used to confirm different properties of the compounds. The Cu(II) complex was characterized by using FTIR, ¹H-NMR, UV-Vis, TGA, DSC, OPM and magnetic susceptibility. FTIR and ¹H-NMR spectroscopy helped confirm the structure for both Schiff base ligand and its complexes, while UV-Vis spectroscopy confirmed the geometry of the CuL and CuLC₁₀ complexes. Magnetic susceptibility tests helped determine magnetic properties and whether the CuLC₁₀ complex contains metal ions and is mononuclear or dinuclear, as well as its paramagnetic, diamagnetic, or ferromagnetic properties. TGA was used to determine the thermal stability of the complex and to confirm its structure by measuring weight loss at different temperatures. Finally, DSC and OPM helped us understand the mesomorphism behavior of the complex.

Based on the FTIR and ¹H-NMR spectroscopy, the synthesis of free Schiff base ligand H₂L was successful. From the FTIR spectrum, the strong

characteristic bands of the $(\text{C}=\text{N})_{\text{imine}}$ functional groups was observed at 1638 cm^{-1} and (O-H) band appear was as broad bands at 2555 cm^{-1} which further indication that a significant hydrogen bond exists between the hydroxyl group (O-H) and the azomethine group (C=N) shows the presence of azomethine group in the Schiff base ligand H_2L . As for $^1\text{H-NMR}$ spectra shows broad signals measured at 13.66 and 9.67 ppm explained the presence of phenolic OH-A and OH-B, respectively. The singlet at 8.36 ppm, shows the presence of the imine moiety (H-C) while signals in the range of 6.16–7.17 ppm shows the presence of the aromatic protons of the salen ligand.

The synthesise of CuL and CuLC_{10} complex structures were identified using FTIR spectrum where both complexes shows strong peaks the strong stretching peak of the $(\text{C}=\text{N})$ at 1604 cm^{-1} and 1619 cm^{-1} for CuL and CuLC_{10} complex respectively which shifted to lower wavelength in compare to free ligand H_2L indicating the coordination of azomethine group with Cu(II) metal. As for the (O-H) for phenolic group it shows a broad band peak of the (O-H) moieties can be observed at 3442 cm^{-1} and 3447 cm^{-1} for CuL and CuLC_{10} respectively which is shifted toward higher wavelength in compared to free ligand H_2L indicating no strong intramolecular hydrogen bond between (O-H) and $(\text{C}=\text{N})$ bonds but instead indicating the coordination of coordination of $(\text{C}=\text{N})$ with Cu(II) ion for both complexes. Besides, the acetate ions peaks also can be observed in the spectra for both CuL and CuLC_{10} complexes for both deprotonated carboxylic group of

acetate asymmetric and symmetric stretching of COO. The CuL recorded peaks at 1541 cm^{-1} and 1448 cm^{-1} acetate asymmetric and symmetric stretching of COO respectively. While, for CuLC₁₀ complex shows acetate asymmetric and symmetric stretching of COO at 1541 cm^{-1} and 1449 cm^{-1} respectively. The Δ value of COO peaks for CuL and CuLC₁₀ complexes were 93 cm^{-1} and 92 cm^{-1} respectively which indicate the chelating binding mode for the acetate ion CH₃COO⁻ for both complexes. However, based on the FTIR spectra of CuLC₁₀ complex indicating no presence of long alkyl chain, decane (C₁₀) and its alkoxy group coordinated to the complex. The geometry of both CuL and CuLC₁₀ confirmed through the UV-Vis spectra that shows a broad *d-d* band at 610 nm ($\epsilon_{max} = 663\text{ M}^{-1}\text{ cm}^{-1}$) that suggesting a square planar structure for Cu(II) centre for both complex. The Schiff base ligand was not able to be analyze using UV-Vis spectroscopy due to the limited amount of product obtained for analysis that caused by limited amount of chemical source for the synthesis reaction such as 2,4-dihydroxy benzaldehyde.

As for the TGA result for the CuLC₁₀ complex. the thermal stability of the complex was only up to 64°C. The decomposition of the complex structure starts with two acetate ions followed by the ligand L. The amount of residue at temperature above 679°C which was 29.07% was in good agreement with the calculated value which was 29.2% by assuming the decomposition for two pure CuO molecules. From the TGA result and calculated values, the

decomposition of the complex shows no involvement of decomposition of long alkyl chain (C_{10}) in the structure which confirmed no coordination of the complex with long alkyl chain (C_{10}). Moreover, the residue for the decomposition of two pure CuO molecules predicted in the TGA shows the existence of two Cu(II) as metal centre in the complex which further confirmed by the magnetic susceptibility analysis of the complex where the effective magnetic moment (μ_{eff}) calculated for the sample was 3.005 BM at 298 K that is a good agreement with expected spin-only value calculated, 2.83 BM for two Cu(II) centres in the complex (2 unpaired electron). This confirmed the CuLC_{10} complex was a dinuclear complex with two Cu(II) metals as centre.

The DSC spectrum shows only an endothermic peak upon heating from 152.0°C to 165.3°C ($\Delta H = 50.57 \text{ kJ mol}^{-1}$) for the melting temperature for CuLC_{10} complex and no peak recorded upon cooling. This shows no indication of liquid crystalline phases from enthalpy data of the DSC analysis. This further confirmed by OPM where no mesomorphism optical textures or birefringence for CuLC_{10} complex instead only shows the small changes in the optical texture of the complex upon heating above 150°C due to melting. The CuLC_{10} complex can be conclude does not exhibit any mesomorphism behaviour based on the DSC and OPM analysis. This may due to the unsuccessful of the synthesis of CuLC_{10} complex in the reaction of CuL complex with 1-bromodecane in the ethanol as solution. Based on

FTIR, TGA and DSC analysis, there were no indication of the CuLC₁₀ complex coordinated with long alkyl chain, decane (C₁₀) causing the complex not to exhibit the mesomorphism behaviour as predicted.

5.2 Suggestion for future works

The synthesis of the Cu(II) complex with long alkyl chain with 1-bromodecane to produce Cu(II) complex with the long terminal end alkoxy group as substituent such as decane with ten carbon chain (long alkyloxy tail) are suggested to use DMF as a solvent instead of ethanol. This is because in this project of synthesis of Cu(II) complex with long alkyl chain as a long alkyloxy substitute tail in the complex as shows in Figure 5.1 involved the Williamson ether synthesis reaction.

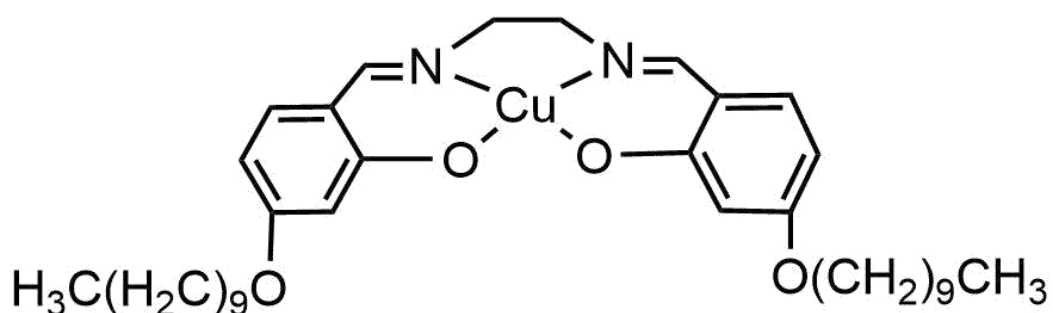


Figure 5.1 The suggested structure for Cu(II) complex with long alkyloxy chain substitute as a long alkyl chain tail for the complex by synthesis reaction of Cu(II) complex with 1-bromodecane

The Williamson ether synthesis reaction is a $\text{S}_{\text{N}}2$ reaction that involves an alkoxide ion that acts as a nucleophile (Ouellette & Rawn, 2015). During this reaction, an alkyl halide is converted into an ether through the displacement of a halide ion by an alkoxide ion (Ouellette & Rawn, 2015). Similarly in this project, the Cu(II) complex that already coordinated with Schiff base ligand H_2L is being reacted with 1-bromododecane (compound with halide ion) to produce complex with ether group (alkyloxy chain tail with C_{10}). In this reaction DMF is suggested to be a good solvent because of its polarity. Since DMF is a polar solvent, it is a good solvent in solvating the transition state that is made in the $\text{S}_{\text{N}}2$ reaction.

Besides, as DMF is also an aprotic solvent, it does not make the nucleophile less attractive, which in this case, is an alkoxide ion. This makes it the best choice for $\text{S}_{\text{N}}2$ reactions that start with the formation of a transition state. By using DMF, the success rate of the Williamson ether synthesis reaction ($\text{S}_{\text{N}}2$ reaction) is higher as the alkoxide ion (nucleophile) can effectively substitute the halide ion and thus produce alkyloxy chain tail substitute (ether group or alkoxy group) by binding the Cu(II) complex with long alkyl chain from 1-bromododecane. Although DMSO is also a polar aprotic solvent, it is less suitable to be used as a solvent for the synthesis as it has a higher boiling point in comparison to DMF, making it harder to be removed after the reaction.

Another suggestion that can be made is to use branched alkyl chains as a substitute at the aromatic ring for the Schiff base other than just a long linear alkyloxy chain to increase the rigidity at the same time, preserve the elongated chain of Schiff base complex. This is because it has been suggested that this can make the structure of the Schiff base complex exhibit mesomorphism behaviour. For example, a study on Pd(II) Schiff base complex with decyloxy as elongated terminal alkoxy group and 2-ethylhexyl as branched terminal alkoxy group had showed optical texture on OPM while showed both SmA and SmC phases at around 40°C on DSC (Iliş et al., 2014).

CITED REFERENCES

- Aazam, E. S., El Hussein, A. F., & Al-Amri, H. M. (2012). Synthesis and photoluminescent properties of a Schiff-base ligand and its mononuclear Zn(II), Cd(II), Cu(II), Ni(II) and Pd(II) metal complexes. *Arabian Journal of Chemistry*, 5(1), 45-53.
- Aswini Krishna, R., Boopathi, T. S., & Senthil, S. (2019). Synthesis and Characterisation of Heterocyclic Metallomesogen. *Materials Today: Proceedings*, 18, 1670-1677.
- Bala, R., Sindhu, R. K., Kaundle, B., Madaan, R., & Cavalu, S. (2021). The prospective of liquid crystals in nano formulations for drug delivery systems. *Journal of Molecular Structure*, 1245, 131117.
- Bartyzel, A. (2017). Synthesis, thermal study and some properties of N₂O₄—donor Schiff base and its Mn(III), Co(II), Ni(II), Cu(II) and Zn(II) complexes. *Journal of Thermal Analysis and Calorimetry*, 127(3), 2133-2147.
- Carlescu, I. (2019). Introductory Chapter: Liquid Crystals. In.
- Cuerva, C., Cano, M., & Lodeiro, C. (2021a). Advanced Functional Luminescent Metallomesogens: The Key Role of the Metal Center. *Chemical Reviews*, 121(20), 12966-13010.
- Cuerva, C., Cano, M., & Lodeiro, C. (2021b). Advanced Functional Luminescent Metallomesogens: The Key Role of the Metal Center. *Chemical Reviews*, 121.
- de Berg, K. C., & Chapman, K. J. (2001). Determination of the Magnetic Moments of Transition Metal Complexes Using Rare Earth Magnets. *Journal of Chemical Education*, 78(5), 670.
- Derkach, L. G., Teslyuk, O. I., Novikova, N. S., Doga, P. G., Yarkova, M. Y., & Meshkova, S. B. (2014). Synthesis of new derivatives of 2,4-dihydroxybenzoic acid and aldehyde and the study of the spectral-luminescent properties of their lanthanide complexes. *Russian Journal of General Chemistry*, 84(7), 1293-1298.
- Dierking, I. (2019). Chapter 1 Introduction. In *Polymer-modified Liquid Crystals* (pp. 1-18). The Royal Society of Chemistry.
- Farhan, N., Said, N., & Binti, R. (2015). *Synthesis characterization and magnetic properties with mesogenic of single molecule copper II palmitate with 2 2 bipyridine and 44 bipyridine.*

- Guo, Y., Hu, X., Zhang, X., Pu, X., & Wang, Y. (2019). The synthesis of a Cu(II) Schiff base complex using a bidentate N₂O₂ donor ligand: crystal structure, photophysical properties, and antibacterial activities [10.1039/C9RA07298E]. *RSC Advances*, 9(71), 41737-41744.
- Hagar, M., Ahmed, H. A., & Saad, G. R. (2018). Mesophase stability of new Schiff base ester liquid crystals with different polar substituents. *Liquid Crystals*, 45(9), 1324-1332.
- Halid, Y. Y. (2016). *Photonic, Magnetic and Metallomesogenic Properties of Cu(II), Ni(II), Co(II), Fe(II) and Mn(II)/Mn(III) Complexes with Alkylcarboxylates, Schiff Bases and Cyclam as Ligands*. Jabatan Kimia, Fakulti Sains, Universiti Malaya. <https://books.google.com.my/books?id=RMennQAACAAJ>
- Hosseinzadeh Sanatkar, T., Khorshidi, A., Sohoul, E., & Janczak, J. (2020). Synthesis, crystal structure, and characterization of two Cu(II) and Ni(II) complexes of a tetradentate N₂O₂ Schiff base ligand and their application in fabrication of a hydrazine electrochemical sensor. *Inorganica Chimica Acta*, 506, 119537.
- Iliş, M., Micutz, M., Dumitraşcu, F., Pasuk, I., Molard, Y., Roisnel, T., & Circu, V. (2014). Enhancement of smectic C mesophase stability by using branched alkyl chains in the auxiliary ligands of luminescent Pt(II) and Pd(II) complexes. *Polyhedron*, 69, 31–39.
- Jadhav, S., & Kapadnis, K. (2018). *Synthesis and Characterization of Schiff bases of Benzaldehyde with Nitroanilines and their Cobalt, Nickel and Copper metal Complexes*.
- Malik, M., Iqbal, M., Shahid, W., Zaheer, S., Din, U., Ikram, M., Anwar, N., Shahid, S., & Idrees, F. (2022). Overview of Liquid Crystal Research: Computational Advancements, Challenges, Future Prospects and Applications. In.
- Mat, A. N. C., & Mohamadin, M. I. (2020). Bis(p-aminobenzoato)bis(hexadecanoato)dicopper(II): A lowtemperature and thermally-stable functional metallomesogen. *Malaysian Journal of Fundamental and Applied Sciences*, 16(6), 597-601.
- Mohammad Isa, M. (2011). *Copper (II) arylcarboxylates : Substituent effects on structure, thermal properties, magnetism, redox and carbon-carbon bond-forming reaction of carbonyls / Mohammad Isa Mohamadin* http://studentsrepo.um.edu.my/12581/1/Mohammad_Isa.pdf
- More, M. S., Joshi, P. G., Mishra, Y. K., & Khanna, P. K. (2019). Metal complexes driven from Schiff bases and semicarbazones for biomedical and allied applications: a review. *Materials Today. Chemistry*, 14, 100195 - 100195.

- Mustafa, S., & AlSharif, M. (2018). Copper (Cu) an Essential Redox-Active Transition Metal in Living System—A Review Article. *American Journal of Analytical Chemistry*, *09*, 15-26.
- Nakum, K., Katariya, K., & Jadeja, R. (2020). Synthesis, characterization, and mesomorphic properties of some new Schiff base homologues series and their Cu(II) complexes. *Molecular Crystals and Liquid Crystals*, *708*, 1-13.
- Ouellette, R. J., & Rawn, J. D. (2015). 16 - Ethers and Epoxides. In R. J. Ouellette & J. D. Rawn (Eds.), *Organic Chemistry Study Guide* (pp. 277-297). Elsevier.
- Ozair, L. N., Mohd Redwan, F., Mohd. Yamin, B., Azizi, F. A., Mustafani, M. S., Nasir, M. S., Hasan, N. H., & Yahya, M. A. (2019). Synthesis and Mesomorphic Studies of Copper(II) with Carboxylato and N-Donor Ligands. *Malaysian Journal of Science Health & Technology*, *4*(Special Issue).
- Parker, R. R., McEllin, A. J., Zeng, X., Lynam, J. M., & Bruce, D. W. (2021). Observation of a frustrated nematic phase in amphiphilic, disc-like complexes of gold(III) containing hydrocarbon and semiperfluorocarbon terminal chains. *Liquid Crystals*, 1-12.
- Pelzl, G., Wirth, I., & Weissflog, W. (2001). The first 'banana phase' found in an original Vorländer substance. *Liquid Crystals*, *28*(7), 969-972.
- Pramanik, H. A. R., Chanda, S., Bhattacharjee, C. R., Paul, P. C., Mondal, P., Prasad, S. K., & Shankar Rao, D. S. (2016). Iron(III) metallomesogen of [N2O2] donor Schiff base ligand containing 4-substituted alkoxy chains. *Liquid Crystals*, *43*(11), 1606-1615.
- Raczuk, E., Dmochowska, B., Samaszko-Fiertek, J., & Madaj, J. (2022). Different Schiff Bases-Structure, Importance and Classification. *Molecules (Basel, Switzerland)*, *27*(3), 787.
- Sadia, M., Khan, J., Naz, R., Zahoor, M., Wadood Ali Shah, S., Ullah, R., Naz, S., Bari, A., Majid Mahmood, H., Saeed Ali, S., Ansari, S. A., & Sohaib, M. (2021). Schiff base ligand L synthesis and its evaluation as anticancer and antidepressant agent. *Journal of King Saud University - Science*, *33*(2), 101331.
- Shanmuga Bharathi, K., Sreedaran, S., Kalilur Rahiman, A., Rajesh, K., & Narayanan, V. (2007). Synthesis, spectral, magnetic, electrochemical and kinetic studies of copper(II), nickel(II) and zinc(II) acetate complexes derived from phenol based 'end-off' ligands: Effect of p-substituents. *Polyhedron*, *26*(14), 3993-4002.

- Ula, S. W., Traugutt, N. A., Volpe, R. H., Patel, R. R., Yu, K., & Yakacki, C. M. (2018). Liquid crystal elastomers: an introduction and review of emerging technologies. *Liquid Crystals Reviews*, 6(1), 78-107.
- Yusuf, T. L., Oladipo, S. D., Zamisa, S. J., Kumalo, H. M., Lawal, I. A., Lawal, M. M., & Mabuba, N. (2021). Design of New Schiff-Base Copper(II) Complexes: Synthesis, Crystal Structures, DFT Study, and Binding Potency toward Cytochrome P450 3A4. *ACS Omega*, 6, 13704 - 13718.

CURRICULUM VITAE

A. Personal profile

Full name Nur Syaza Sahira Binti Ahmad Zaidi
National IC no 990406-13-6086
Birth date 6th April 1999
Citizenship Malaysia
Place of birth Sibu, Sarawak
Gender Female
Correspondence address No, 62, Lorong 7B5 Siol Kandis, Taman Tatai Kumang, Jalan Demak, 93050 Petra Jaya, Kuching, Sarawak, Malaysia
Telephone no (HP) 013-5762928
Email address nursyazazaida@gmail.com / 2020988343@student.uitm.edu.my



B. Hobbies and interests

I enjoy reading, travelling and exploring places. I like to meet new people, learn about cultures and the arts and learn new things. I listen to light and easy music and enjoy classical Malay music.

I am very fluent in written and spoken Malay and English and have basic knowledge of Arabic and Mandarin.

C. Academic qualifications

Degree	Area	Institution	Year awarded
B.Sc. (Hons.)	Chemistry with Management	Universiti Teknologi MARA, Malaysia	2023
Diploma	Science	Universiti Teknologi MARA, Malaysia	2020
SPM	Science	SMKA Shiekh Haji Othman Abdul Wahab	2017

D. Related experience

Post	Place	Year
Vice President	CHEMISTS Committee, Universiti Teknologi MARA, Malaysia	2022-2023
Moderator	Inbound, Outbound mobility program with Japan, Universiti Teknologi MARA, Malaysia	2022

Participant	Innostre, BCCK	2022
Committee	CHEMISTS Committee, Universiti Teknologi MARA, Malaysia	2021- 2022
Committee	Doctor Muda Club, SMKA Shiekh Haji Othman Abdul Wahab	2015- 2016

E. Awards

Post	Place	Year
Certificate	Dean's List Award 2018,Universiti Teknologi MARA, Malaysia	Mar 2018
Certificate	Dean's List Award 2018,Universiti Teknologi MARA, Malaysia	Oct 2018
Certificate	Dean's List Award 2018,Universiti Teknologi MARA, Malaysia	Mar 2019
Certificate	Dean's List Award 2018,Universiti Teknologi MARA, Malaysia	Oct 2019
Certificate	Dean's List Award 2018,Universiti Teknologi MARA, Malaysia	Mar 2020
Certificate	Dean's List Award 2018,Universiti Teknologi MARA, Malaysia	Mar 2022